Centrosomal P4.1-associated protein (CPAP) is a novel regulator of ESCRT pathway function during multivesicular body formation and endosome maturation

Radhika Gudi [#*] and Chenthamarakshan Vasu[#]

[#]Department of Pharmacology and Immunology, College of Medicine, Medical University of South Carolina, Charleston, SC 29425

*Corresponding author: gudi@musc.edu

Short title**: CPAP regulates ESCRT function and endosome maturation**

Abstract:

Previously, we have shown that Centrosomal P4.1-associated protein (CPAP) is a positive regulator of endocytic vesicle transport (EVT) pathway, and it promotes lysosomal targeting of ligand-bound EGFR. Here, we show that recruitment of TSG101, an ESCRT-I protein, to endosome is the mechanism by which CPAP facilitates EVT. While CPAP depletion disrupts the Rab5-to-Rab7 conversion and endosome maturation processes, it does not interact with these GTPases. We found that CPAP not only co-immunoprecipitates with TSG101, but also colocalizes with TSG101 as well as ESCRT 0 protein HRS on the early endosomes. Although CPAP-TSG101 interaction occurs under quiescent state, this interaction is more robust during EVT progression. TSG101 recruitment to endosome and Rab5-to-Rab7 conversion were restored in CPAP depleted cells upon overexpression of HRS suggesting that CPAP functions upstream of TSG101, but in parallel to HRS, and bridges ESCRT 0 and ESCRT I components. Our results reveal a novel ESCRT dependent regulatory role for the centriole biogenesis protein CPAP in endosome maturation.

Teaser: Microcephaly-associated protein CPAP recruits TSG101 to the endosome and facilitates ESCRT function and endosome maturation.

Key words: CPAP, endosomal trafficking, endocytic vesicular transport, EVT, ESCRT, TSG101, HRS, MVB biogenesis, endosome maturation, Rab5-to-Rab7 conversion, EGFR.

Introduction:

The endosomal trafficking/endocytic vesicular transport (EVT) pathway involves precisely coordinated signaling events that originate at the endosomes and post-endocytosis at the plasma membrane. This pathway is critical for inter-and intra-cellular communication as well as to regulate the abundance and function of proteins including cell surface receptors (*1-6*). Upon endocytosis, internalized cargo such as ligand-bound epidermal growth factor receptor (EGFR) at the plasma membrane, is first routed to the early endosomes. These vesicular structures serve as a sorting hub for endocytosed cargo and play a major role in deciding its fate. Endocytosed cargo can undergo recycling back to the surface, degradation in the lysosome, and/or release in exosomes(*1, 7-9*). Formation of an intraluminal vesicle (ILV) packed intermediate endocytic organelle, referred to as the multi-vesicular body (MVB) or the late endosome (LE) (*10, 11*), and the sequential acquisition and activation of GTPases Rab5 and Rab7 on to early endosome during endosome maturation (*12-14*) are the key events that precede lysosome targeting of the endocytosed cargo.

Rab5-to-Rab7 conversion, a process involving the recruitment of Rab7 onto Rab5 positive vesicles and replacement of Rab5 with Rab7, is an important step that marks the maturation of EE to MVBs or LE (*15, 16*). ILV that is an essential component of MVBs are generated in an endosomal sorting complex for recruitment and transport (ESCRT) pathway dependent manner. ESCRT is composed of several sub-complexes: ESCRT-0, ESCRT-I, ESCRT-II and ESCRT-III. Among these ESCRT complexes, HRS (ESCRT-0) and TSG101 (ESCRT-I) are the initiators of MVB biogenesis (*17-19*). In addition, several accessory proteins such as ALIX, LIP5 and ATPases such as VPS4B are also essential for the function of ESCRT pathway (*20*). However, although both are essential for EVT to proceed unhindered, whether Rab5-to-Rab7 conversion and ESCRT function are sequential or parallel events and if these pathways coordinate during cargo transport are largely unknown.

Previously, we have reported the novel, positive regulatory function of CPAP (Centrosomal P4.1 associated protein; expressed by CENPJ gene)/SAS-4, a microtubule/tubulin binding essential centriole biogenesis protein (*21-24*) during EVT of internalized EGFR cargo (*25*). Prior to this report, CPAP function has been primarily attributed to its role during centriole duplication, specifically restricting the centriole length, and ciliogenesis (*21, 24, 26-30*). CPAP regulates

microtubule growth to produce centrioles of optimum dimension (*31*). Employing gain- and loss-of-function approaches as well as the ligand-bound EGFR intracellular-trafficking model, we demonstrated that CPAP is required for efficient transport of internalized EGFR to MVB and lysosome for degradation. Depletion of CPAP resulted in disruption of MVB formation and lysosome targeting of ligand-bound EGFR, causing increased cellular abundance and constitutive signaling by this receptor (*25*). Importantly, higher EGFR levels and defective EVT function due to CPAP-deficiency were correlated with increased tumorigenicity of oral cancer cells (*32*). These reports demonstrated that CPAP has a positive regulatory role in MVB biogenesis and EVT of receptor cargo for degradation.

Here, we have investigated the potential molecular mechanisms by which CPAP positively regulates EVT. We found that Rab5-to-Rab7 conversion, which facilitates endosome maturation and the ESCRT pathway function and triggers ILV production are both compromised in CPAP-depleted cells, explaining the MVB formation defects in CPAP deficient cells that we reported previously (*25*). Specifically, we have identified an interaction between CPAP and the ESCRT-I protein TSG101, and this functional interaction is more profound during endocytic trafficking. Interestingly, CPAP not only localizes to the endosome, co-localizes with ESCRT-0 protein HRS and TSG101, but it is also required for recruiting TSG101 to the endosomes during ligand induced EVT of EGFR. Overexpression of HRS, but not TSG101 itself, compensates for CPAP function in terms of TSG101 recruitment to endosome, Rab5-Rab7 conversion, endosome maturation and EVT of EGFR. Our data suggests that CPAP is a critical component of the ESCRT pathway, and it bridges ESCRT-0 and ESCRT-I functions on the endosomes, early, during MVB biogenesis.

Results:

CPAP-depletion does not affect Rab5 recruitment to the endosome

Our previous report (*25*) showed a novel function for CPAP in positively regulating EVT. Using EGFR as a model to study EVT and lysosomal targeting of endocytosed receptor, we demonstrated that MVB biogenesis and the late endosome sorting of cargo targeted for lysosomal degradation, as indicated by the lack of localization of internalized EGFR in MVBs, are defective in CPAP deficient cells. We found that CPAP depletion resulted in increased cellular levels of total and

phospho-EGFR suggesting sustained EGFR signaling, and reintroduction of CPAP expression restored EVT and EGFR homeostasis. Therefore, here, we sought to understand the mechanism by which CPAP impacts the vesicular transport pathway, by specifically addressing how the transport of EGFR between early and late endosomes is regulated.

Rab5 and Rab7, small molecular weight guanine triphosphatases (GTPases) that function in the tethering/docking of vesicles to their target compartment, are sequentially recruited to the early endosomes. This temporally regulated recruitment plays a critical role in endosome maturation and the transport of endocytosed receptor cargo towards the late endosomes/lysosomes for degradation (*15*). Therefore, to begin to understand why CPAP-depleted cells fail to form MVB and target the receptor cargo to late endosomes, we examined if cellular levels of Rab5 and Rab7 proteins are affected upon CPAP depletion. Immunoblotting (IB) assay of HeLa cells stably expressing control-shRNA and CPAP-specific shRNA (CPAP-knockdown) showed comparable levels of Rab5 and Rab7 proteins **(Supplemental Fig. 1)** suggesting that CPAP depletion has no impact on the cellular levels of these Rab proteins. Then, using Alexa fluor 555-linked EGF (AF555-EGF), we studied if recruitment of Rab5 to endosomes and the trafficking of ligand-bound EGFR to Rab5 positive vesicular structures are impacted upon CPAP depletion. Confocal microscopy analysis showed, upon EGF treatment, comparable degree of Rab5 recruitment to endosomes and colocalization with EEA1 and CD63 positive vesicular structures in both control and CPAP depleted cells **(Fig. 1A&B)**. Furthermore, both maximum projection and single Z-scan images showed that colocalization of internalized AF555-EGF with Rab5 was not considerably different at the two time-points tested **(Fig. 1C)**, suggesting that CPAP depletion does not affect Rab5 recruitment or early stages of EVT pathway. Of note, confocal microscopy images showed no difference in the relative fluorescence intensity of Rab5 between the control and CPAP-depleted cells confirming that Rab5 levels or function are not influenced by CPAP.

CPAP-depletion diminishes Rab7 recruitment to the endosome

During endosome maturation and cargo sorting for MVB formation, Rab7 is recruited to the maturing endosome and replaces Rab5 (referred to as the Rab5-to-Rab7 conversion) in a highly coordinated manner (*15*). Therefore, we determined if Rab7 recruitment to endosome and ligand bound EGFR localization on Rab7 positive endosomes is dysregulated in CPAP depleted cells. Control and CPAP-depleted HeLa cells were examined for localization of Rab7 on early and late

endosomes upon EGF treatment. We found that Rab7 colocalization with EEA1 and CD63 positive vesicular structures was lower in CPAP depleted cells compared to control cells **(Fig. 2A&B)**. Cells treated with AF555-EGF were also stained with Rab7 to determine if the ligand bound EGFR cargo is transported to Rab7 positive late endosomes. Both maximum projection and single Z-scan images show that ligand bound EGFR localization on Rab7 positive vesicles was significantly lower in CPAP depleted cells compared to control cells, at both time points tested **(Fig. 2C)**. Furthermore, perinuclear clustering of Rab7 was visibly diminished in these cells upon CPAP depletion. Importantly, although the IB assay showed cellular expression levels of Rab7 were unaffected by CPAP depletion **(Supplemental Fig. 1),** the relative fluorescence intensity of Rab7 in CPAP-depleted cells after ligand binding was significantly lower, suggesting its reduced clustering on vesicular structures during EVT progression **(Fig. 2C).** These observations suggest a defect in the activation and recruitment of Rab7 to the endosomes under CPAP deficiency. These results also suggest that our observation of failed transport of ligand bound EGFR to the MVBs and lysosomes (*25*) is, at least in part, due to the failure in recruiting Rab7 to endosomes, resulting in diminished endosome maturation.

CPAP depletion disrupts Rab5-to-Rab7 conversion

Since we found that Rab7 recruitment to endosome is defective in CPAP depleted cells, we used Airyscan super-resolution microscopy to determine if receptor internalization induced endocytic vesicular colocalization of Rab5 and Rab7 is impacted when CPAP is depleted. We employed both shRNA and siRNA approaches **(Supplemental Figs. 1&2)** that were validated in our previous reports (*25, 32*). Control and CPAP-depleted HeLa cells were treated with untagged EGF, stained, and imaged to detect Rab5 and Rab7 colocalization. Both maximum intensity projection and single Z images showed that colocalization of Rab7 with Rab5 was significantly lower in CPAP-depleted cells **(Fig. 3A and Supplemental Fig. 3)**, indicating that Rab7 recruitment to Rab5 positive endosomes and Rab5-to-Rab7 conversion is disrupted in the absence of CPAP.

Since CPAP depleted cells show diminished recruitment of Rab7 to endosomes during EGFR trafficking and lower overall Rab7 staining intensity **(Fig. 2)**, we examined if overexpression of Rab7 restores endosome maturation and the EVT of endocytosed EGFR to MVBs. Control and CPAP depleted HeLa cells were transfected with vector constructs encoding cDNA for GFP-Rab7, either wild-type (WT) or dominant negative (DN) and subjected to EGFR trafficking assay using

AF555-EGF followed by confocal imaging. CPAP depleted cells, as expected, showed lower degree of localization of ligand bound EGFR to the CD63 positive late endosome/MVBs compared to control cells **(Fig. 3B)**. Importantly, overexpression of WT Rab7 restored EGFR trafficking to MVB in CPAP depleted cells as indicated by the localization of AF555-EGF to the CD63 positive vesicular structures. However, exogenous expression of DN Rab7 not only failed to restore the EVT of EGFR, but also suppressed the MVB localization of AF555-EGF in control cells. These results substantiate an important role for Rab7 recruitment to endosome in CPAP mediated positive regulation of EVT and trafficking of ligand bound EGFR to MVB. Further, this data also suggests that CPAP functions at the level of, by direct interaction, or upstream of Rab7 recruitment to facilitate EVT. In this regard, we conducted an immunoprecipitation (IP) assay using lysates of GFP, GFP-Rab5 or GFP-Rab7 expressing cells to determine if Rab5 and Rab7 interact with CPAP. Immunoblotting of GFP specific pulldown suggested no interactions between CPAP and these Rab proteins **(Supplemental Fig. 4)**. This lack of CPAP-Rab7 interaction suggests that although endosome maturation and Rab7 recruitment to the endosome is affected upon CPAP depletion, another mechanism or player that operates in parallel or upstream of Rab5-to-Rab7 conversion could be the target of CPAP mediated positive regulation of EVT.

Recruitment of TSG101, an ESCRT-I component, to the endosomes is compromised in CPAP depleted cells

Endosome maturation is concomitantly regulated by the Rab GTPases and ESCRT complexes, especially during the early to late endosome transition. ESCRT proteins (0, I, II, III and its accessory counterparts) are sequentially recruited to the early endosome membrane and they drive the inward bending of cargo-associated membrane to generate ILVs that form the mature MVB (*20, 33*). These ILV-rich MVBs fuse with lysosomes to form endolysosomes and degrade the endocytosed receptor cargo. Importantly, ESCRT disruption has been reported to inhibit the completion of Rab5-to-Rab7 conversion (*34*). Further, endocytic cargo corralling by ESCRTs upstream of Rab5-Rab7 conversion has been hypothesized in a recent study (*35*). Nevertheless, coordination of ESCRT and Rab5-to-Rab7 conversion pathways during endosome maturation and MVB formation is not understood. Here, we tested the dynamics of ESCRT function during the EVT of EGFR in control and CPAP-depleted HeLa cells. To determine ESCRT recruitment to endosomes, EGF-treated cells were stained using HRS (ESCRT-0), TSG101 (ESCRT-I) and ALIX

(ESCRT accessory component) specific antibodies together with the anti-EEA1 antibody and subjected to Airyscan super-resolution microscopy. Of note, specificities of the ESCRT component antibodies were confirmed by immunoblotting and immunofluorescence of control and specific siRNA treated cells **(Supplemental Fig. 5A&B)**. Importantly, we found that the recruitment of HRS or ALIX to the EEA1 positive vesicular structures (early endosomes), as assessed by quantifying the number of colocalized puncta, was not different between control and CPAP-depleted cells **(Fig. 4)**. However, the localization of TSG101, an ESCRT-I component, which triggers MVB formation and downstream EVT events (*18*), on the early endosomes was significantly lower in CPAP-depleted cells when compared to control cells, suggesting that CPAP may be required for TSG101 recruitment to the endosome. Importantly, it has been shown before that ESCRT-0 protein HRS triggers TSG101 localization/recruitment to the endosomes (*17*). Our experiment using HeLa cells to re-assess this aspect showed that TSG101 recruitment to the early endosomes during EGF treatment is, in fact, diminished severely in HRS depleted cells **(Supplemental Fig. 6)**. These observations suggest that CPAP and HRS function similarly, in terms of TSG101 recruitment during EVT.

An increase in CPAP localization to the early endosomes and colocalization with HRS and TSG101 is observed during EVT progression

Since CPAP depletion appears to disrupt TSG101 recruitment to the early endosome, employing different approaches and multiple EEA1 antibodies, we examined if CPAP localizes to early endosome under quiescent state and upon EVT progression. Control and CPAP depleted cells were left untreated or treated with EGF and subjected to immunostaining for CPAP and EEA1 followed by confocal microscopy. As observed in **Supplemental Fig. 7**, considerable proportion of EEA1 positive vesicular structures were also positive for CPAP staining in quiescent and EGF stimulated cells. Localization of CPAP on EEA1 positive puncta was significantly diminished in CPAP depleted cells showing the specificity of endosomal staining of CPAP. We have then examined if CPAP colocalizes with TSG101 and HRS on early endosomes. Control and EGF treated cells were stained for EEA1 and CPAP, alone or along with HRS and TSG101, and subjected to Leica Lightning-based super resolution microscopy. As observed in **Fig. 5A**, CPAP colocalizes with EEA1 positive puncta in untreated cells, and shows a significant time-dependent increase in this colocalization during EVT progression in EGF treated cells. Examination of tri-protein

colocalization, CPAP and HRS or CPAP and TSG101 on EEA1 positive vesicular structures, also revealed that CPAP along with these ESCRT proteins localizes to the early endosomes during EVT progression. While CPAP and ESCRT proteins (HRS and TSG101) were found to be colocalized to a small number of EEA1 positive vesicular structures in untreated cells, this tri-protein colocalization showed a time-dependent increase in EGF treated cells **(Fig. 5B)**. Overall, these observations suggest that CPAP is recruited to the early endosome, along with ESCRT-0 and ESCRT-I proteins, during EVT of cell surface receptor cargo.

To substantiate the observation that CPAP localizes to endosome and is actively recruited to vesicular structures during EVT progression, we have examined the presence of CPAP on vesicular structures by IB and transmission electron microscopy (TEM). IB of endosome fraction from CPAP overexpressing (GFP-CPAP) cells showed the presence of CPAP along with Rab5 and Rab7 **(Fig. 5C)**. Further, the endosome fraction of non-transfected, EGF treated cells showed higher levels of endogenous CPAP compared to that of untreated cells **(Fig. 5D)**. TEM images of EGF-treated cell sections that were labeled using CPAP specific antibody followed by gold particle-linked secondary antibody showed positive labelling of vesicular structures for CPAP **(Supplemental Fig. 8A&B**). Overall, these observations confirm the presence of CPAP on early endosomes and its expression gets particularly enriched during EVT progression.

Re-introduction of CPAP expression restored TSG101 recruitment on to early endosome in CPAP and HRS depleted cells

Since we observed that CPAP can localize to the early endosome, it actively colocalizes with ESCRT proteins on early endosome during EVT progression, and its depletion disrupts TSG101 recruitment to the early endosome, we next determined if reintroduction of CPAP expression can restore TSG101 recruitment to the endosome in CPAP and HRS knockdown cells. HeLa cells stably transfected with doxycycline inducible, RNAi-resistant, GFP-tagged-CPAP cDNA were treated with CPAP-specific siRNA to deplete endogenous CPAP expression, induced exogenous GFP-CPAP expression, treated with EGF to induce EVT and subjected to immunostaining with the anti-EEA1 and -TSG101 antibodies for Airyscan-based super-resolution microscopy as depicted in **Fig. 6A.** As expected, CPAP-siRNA and HRS-siRNA treated control cells showed significantly lower colocalization of TSG101 and EEA1 compared to control siRNA treated cells. However, upon induction of GFP-CPAP expression in CPAP-siRNA treated cells, localization of

TSG101 on EEA1 positive vesicular structures was significantly increased **(Fig. 6B)**, suggesting that TSG101 recruitment to endosomes is restored, at least in part, by reintroduction of CPAP. Importantly, overexpression of CPAP in HRS depleted cells, similar to CPAP depleted cells, restored TSG101 recruitment to the early endosomes. Overall, these results suggest that not only the disruptive effect of CPAP knockdown on TSG101 recruitment to the early endosomes during EVT is specific to lowered CPAP levels, but also the previously reported, HRS-mediated recruitment of TSG101 on to endosomes can be compensated by CPAP.

HRS, but not TSG101, overexpression restored TSG101 recruitment onto endosome and EVT function in CPAP-depleted cells

It has been shown that EVT and MVB formation are facilitated by HRS-TSG101 interaction (*17, 19, 36*). Since CPAP-depleted cells are defective in MVB formation and EVT of EGFR (*25*), we tested if overexpression of HRS or TSG101 alone was sufficient to restore TSG101 recruitment to endosomes and trafficking of EGFR to MVBs in these cells. Control and CPAP -siRNA treated HeLa cells were subjected to GFP-TSG101 or HRS expression vector transfection and examined for colocalization of TSG101 on EEA1 positive vesicular structures or trafficking of AF555-EGF to CD63-positive MVBs **(Fig.7A)**. As observed in **Fig. 7B**, no significant increase in the localization of TSG101 on EEA1 positive vesicular structures of CPAP-depleted cells, compared to mock-transfected cells, was observed upon TSG101 overexpression itself. Unlike TSG101-overexpression, HRS-overexpression in CPAP-depleted cells led to significantly higher colocalization of TSG101 on EEA1 positive vesicular structures as compared to mock transfected cells. This suggests that, similar to CPAP's ability to compensate for HRS function **(Fig. 6)**, higher protein levels of HRS can compensate for CPAP function in terms of TSG101 recruitment to the endosome. Further, CPAP functions upstream of TSG101, but appears to be in parallel to HRS in recruiting ESCRT pathway proteins to the endosome and facilitating MVB formation. To validate this notion, EGFR trafficking to MVBs in CPAP-depleted cells that are overexpressing TSG101 or HRS was examined after treating with AF555-EGF. **Fig. 7C** shows that the degree of AF555-EGF localization to CD63 positive vesicular structures was not significantly different in CPAP depleted, TSG101 overexpressing cells as compared to CPAP-depleted cells. On the other hand, AF555-EGF colocalization with CD63 positive vesicular structures was higher in CPAP-depleted, HRS overexpressing cells compared to CPAP depleted controls. Overall, these results, in the

context of our previous report (*25*), show that ESCRT pathway function is disrupted upon CPAP depletion due to failed TSG101 recruitment to early endosomes, leading to defective MVB formation and receptor cargo transport. These results reiterate the notion that CPAP acts upstream of TSG101 and parallel to HRS in the MVB biogenesis pathway.

CPAP depletion does not impact the cellular levels of TSG101

Since CPAP depletion appears to disrupt TSG101 recruitment onto the endosome, we examined whether cellular levels of TSG101 and other key ESCRT proteins are altered upon CPAP depletion. First, lysates of control- or CPAP-depleted HeLa **(Fig. 8A)** and HEK293T **(Fig. 8C)** cells were subjected to immunoblotting to detect HRS, TSG101 and ALIX. Fig. 8A and 8C shows that protein levels of these ESCRT proteins are comparable in control and CPAP depleted cells in both cell lines. Cellular levels of these ESCRT proteins appear to be unaltered in CPAP depleted cells under EGF stimulation as well **(Supplemental Fig. 9)**. We, then, stained control and CPAP depleted HeLa and HEK293T cells to detect intracellular levels of CPAP and TSG101 and analyzed by flow cytometry. This assay also showed that cellular levels of TSG101 remain unaltered by CPAP depletion **(Fig. 8B and 8D)**. These observations, in the context of afore-described disrupted recruitment of TSG101 on to endosome in CPAP depleted cells, suggest that CPAP positively regulates direct or HRS-dependent recruitment of TSG101 onto the endosome, but does not have an influence on the cellular levels or stability of this ESCRT protein during EVT.

CPAP interacts with TSG101, and this interaction is enhanced upon EVT

To begin to understand how CPAP regulates TSG101 recruitment to the endosomes, we tested if the ESCRT proteins interact with CPAP. HEK293T cell lysates were subjected to IP using HRS, ALIX and TSG101 specific antibodies separately, followed by IB to detect these proteins along with CPAP. Interestingly, CPAP was detected in the pull-down of all three ESCRT components **(Fig. 9A)** suggesting that it is associated with ESCRT machinery proteins under quiescent state. To substantiate the observed interaction between CPAP and ESCRT proteins, HEK293T cells stably transfected with inducible GFP-CPAP vector were treated with doxycycline to induce GFP-CPAP expression, left untreated or treated with EGF, and subjected to IP and IB. GFP specific IP of untreated cells probed for ESCRT proteins showed only TSG101, but not HRS or ALIX **(Fig. 9B)**. Surprisingly, the amount of TSG101 pulled down along with GFP-CPAP was profoundly

higher in EGF stimulated cells compared to untreated cells, suggesting that the interaction between CPAP and TSG101 is amplified during the progression of EVT.

HRS-TSG101 interaction is abrogated in the absence of CPAP during EVT

To evaluate the role of CPAP in bridging ESCRT recruitment during EVT, HRS-TSG101 interaction was evaluated in EGF-treated, control or CPAP-depleted cells. While the amount of TSG101 immunoprecipitated from the control and CPAP depleted cells was comparable, IB of these pulldowns with anti-TSG101 antibody revealed a significant reduction in the amount of HRS pulled down from CPAP-depleted cells, as compared to control cells, by TSG101 specific antibody **(Fig. 9C)**. Reciprocal IP of EGF-treated, control or CPAP-depleted cells using HRS antibody showed lower TSG101 protein pulldown from CPAP depleted cells compared to control cells **(Fig. 9D)**. These observations suggest that CPAP is essential for the functional interaction between HRS and TSG101 and the recruitment of TSG101 to endosome by HRS during endocytosed receptor cargo transport.

Rab5-to-Rab7 conversion and EGFR trafficking to lysosome are restored in CPAP-depleted cells upon HRS, but not TSG101, overexpression

Our previous study showed that lysosomal targeting of ligand bound EGFR to lysosome is disrupted upon CPAP depletion (*25*). Our results here show that, although CPAP does not interact with or affect the cellular levels of Rab5 or Rab7, Rab5-to-Rab7 conversion is blocked in CPAP depleted cells **(Fig. 3 and Supplemental Figs 1&3)**. Further, our observations that CPAP not only interacts with TSG101, but also bridges HRS dependent recruitment of TSG101 to endosomes and restores EVT function in CPAP depleted cells **(Figs. 6-9)** suggest that disruption of ESCRT pathway function is responsible for the defective Rab5-to-Rab7 conversion in CPAP depleted cells. Therefore, first we tested if overexpression of ESCRT component, TSG101 or HRS is sufficient to restore Rab5-to-Rab7 conversion. Control and CPAP-siRNA expressing HeLa cells were subjected to GFP-TSG101 or GFP-HRS expression vector transfection and examined for Rab5 and Rab7 colocalization in them using Lightning super-resolution microscopy. As observed in **Fig. 10A**, overexpression of TSG101 in CPAP depleted cells did not increase colocalization of Rab5 and Rab7 as compared to control cells. On the other hand, HRS overexpression in CPAP depleted cells increased the localization of Rab7 onto the Rab5 positive vesicular structures as compared to control cells. This data confirms that CPAP functions in parallel to HRS and Rab5-

to-Rab7 conversion during EVT. Next, we examined if the EVT function and localization of internalized ligand-bound EGFR to Rab7 positive vesicular structures are restored in CPAP depleted cells upon overexpression of TSG101 or HRS. As shown in **Fig. 10B**, HRS overexpression in CPAP-depleted cells caused an increase in the localization of ligand (AF555-EGF) bound EGFR to Rab7 vesicular structures compared to control cells. However, TSG101 overexpression failed to restore transport of ligand bound EGFR to Rab7 vesicles in CPAP depleted cells. Overall, these results, in the context of above-described observation that HRS overexpression restores TSG101 recruitment to endosomes in CPAP-depleted cells, suggest that Rab5-to-Rab7 conversion defects in CPAP depleted cells is due to the failed TSG101 recruitment to early endosome.

Discussion

The EVT, also referred to as endosomal trafficking, process is critical for many cellular functions, including regulation of signaling through cell surface receptors by targeting ligand bound receptors to the lysosome for degradation or recycling back to the plasma membrane. MVBs serve as critical intermediates during this process by sorting the endocytosed cargo and routing these cargo proteins to the lysosome (*37*). In our recent reports (*25*), we have shown a novel positive regulatory role for CPAP, an essential centriole elongation protein (*21, 24, 38*), on MVB biogenesis and lysosome targeting of ligand bound EGFR and downregulating signaling by this receptor. Here, we demonstrate that CPAP positively regulates MVB and lysosomal targeting of endocytosed cargo by facilitating Rab5 to Rab7 conversion and ESCRT protein recruitment, which are both critical steps for early endosome maturation to lysosomes.

Endosomal trafficking of the cell surface receptor cargo is tightly regulated through Rab GTPases such as Rab5 and Rab7. Progression from the early endosome to late endosome, which is composed of MVBs, has been shown to be regulated by a Rab5-to-Rab7 switch involving an exchange between the cytosolic pool and the endosomal membrane-bound fraction of Rab5 and Rab7 (*15*). Completion of endosome maturation generates Rab7 and CD63 positive late endosomes/MVBs (*39, 40*). Our previous report (*25*) showing defective EVT of endocytosed EGFR to late endosome and lysosome in CPAP depleted cells suggested that Rab conversion and/or cellular levels and endosomal recruitment of Rab5 and Rab7 could be impacted upon CPAP

depletion. In fact, we found that while localization of Rab5 to early endosome is comparable in control and CPAP depleted cells, not only the Rab7 recruitment to endosomes is diminished, but also ligand bound EGFR cargo failed to reach the Rab7 positive vesicles. Importantly, Rab5-to-Rab7 conversion, which is indicated by the colocalization of these GTPases on vesicular structures, upon EVT induction using EGF, is severely diminished in CPAP depleted cells. This observation suggested to us that CPAP may be regulating the cellular levels of Rab7 or be involved in recruiting this GTPase to endosome. However, our IB and IP studies showed that CPAP does not interact with either Rab5 or Rab7 and the cellular levels of these GTPases are also not considerably altered upon CPAP depletion suggesting that the suppressive effect of CPAP depletion on Rab5-to-Rab7 conversion, endosome maturation and receptor cargo transport are indirect effects.

Previous studies that used yeast and mammalian cells have shown that the evolutionarily conserved ESCRT-0, -I, -II, and -III complexes act sequentially in receptor sorting and MVB biogenesis. These ESCRT complexes are transiently recruited from the cytoplasm to endosome where they bind to internalized receptors that are marked for degradation by ubiquitination (*41, 42*). HRS (ESCRT-0 protein) and TSG101 (ESCRT-I protein) are known to be functionally important in initiating the endosomal trafficking and MVB biogenesis process (*17-19, 43*). HRS binds to TSG101 and mediates the targeting of ESCRT-I complex to early endosomes (*17*). On the other hand, TSG101 is critical for efficient degradation of EGFR, indicating its essential role in the sorting of cargo in MVBs and trafficking to lysosome (*18*) . ALIX, an ESCRT associated accessory protein, is known to recruit ESCRT-III proteins to endosome during various ESCRT dependent cellular processes including the ubiquitin-independent ILV sorting of G protein–coupled receptors PAR1 and P2Y1 for degradation (*44, 45*). In this regard, although Rab5-to-Rab7 switch is also a critical step of endosome maturation, it is largely unknown how Rab conversion and ESCRT machinery function are coordinated to generate MVBs/late endosomes for trafficking of receptor cargo to lysosome. Since CPAP depletion diminished Rab conversion and endosome maturation, we studied if CPAP deficiency impacts EVT induced endosome localization of key ESCRT proteins. Our data indicate that CPAP acts as a critical intermediary during the recruitment of TSG101 to endosome and perhaps, promotes Rab5-to-Rab7 conversion through ESCRT pathway function.

Although it has been reported that early- and late-acting ESCRTs preferentially localize on early and late endosomes respectively (*46*), it is now established that all ESCRTs can localize to EEA1 positive compartment during stimulation of vesicular transport (*47, 48*). It has also been reported that HRS overexpression can cause accumulation of TSG101 in early endosome supporting the notion that HRS acts early and recruits TSG101 to early endosome membrane during EVT progression (*18, 19*). Our results show that EGF stimulation of cells to induce EVT causes the recruitment of HRS and TSG101, as well as the ESCRT-III associated protein ALIX to early endosomes. Interestingly, we also found that similar to ESCRT proteins, CPAP is localized on to the early endosomes in quiescent cells, and it is actively recruited to and colocalizes with ESCRT proteins on the endosome during EVT progression.

With respect to ESCRT recruitment, we observed that only TSG101, but not HRS or ALIX, localization on early endosome is disrupted in CPAP depleted cells. Importantly, reintroduction of CPAP function restored TSG101 recruitment to the endosome in both CPAP and HRS depleted cells suggesting that CPAP can compensate for HRS function, in terms of TSG101 recruitment to early endosome, during the vesicular transport. Furthermore, overexpression of the upstream ESCRT HRS, but not TSG101 itself, caused restoration of TSG101 localization on early endosome in CPAP depleted cells. Overall, these observations suggests that CPAP acts in parallel to HRS for TSG101 recruitment to endosome during EVT. Our data highlights the essential nature of CPAP function in EVT as CPAP-depleted cells fail to function despite intact cellular and endosomal HRS.

Previous reports have shown that both HRS and TSG101 play key roles in MVB formation and cargo sorting for lysosomal targeting, with HRS being critical for recruiting downstream ESCRT components including TSG101 to endosome. On the other hand, TSG101 primarily functions by recognizing and binding ubiquitinated cargo proteins targeted for lysosomal degradation and promotes the stability of the vacuolar domains within the early endosome from which MVBs originate (*18, 49*). Previous reports showing that depletion of HRS has only a modest effect on EGF degradation, compared with the almost complete inhibition of EGF degradation upon depletion of Tsg101 (*18*) not only validate this notion, but also suggest that MVB/late endosome formation are dependent on highly orchestrated functions of ESCRT components. Hence, our observations that TSG101 recruitment is disrupted in CPAP depleted cells and restored by CPAP

expression in HRS depleted cells indicate that CPAP, at least in part, contributes to TSG101 recruitment to endosome and acts as an integral component of ESCRT machinery. Our results also show that the recruitment of ESCRT-III associated protein ALIX to early endosome is independent of TSG101 recruitment.

HRS-TSG101 and TSG101-ALIX interactions have been reported before (*17, 50*). Our observations on the disrupted TSG101 localization to early endosomes in CPAP depleted cells suggested that CPAP interacts with TSG101 and/or other upstream ESCRT components and/or regulates the cellular levels of these proteins. In this regard, our results show that depletion of CPAP has no impact on the total cellular levels of HRS, TSG101 or ALIX suggesting that the disrupted TSG101 recruitment to endosome is not due to diminished protein levels. Lack of restoration of TSG101 recruitment to early endosome in CPAP depleted cells even upon overexpressing this protein substantiates this notion. More importantly, however, our IP studies showing that CPAP can be immunoprecipitated using HRS, TSG101 and ALIX specific antibodies indicate that endogenous CPAP exists in physiological complex with ESCRT proteins. On the other hand, when exogenously expressed GFP-CPAP was immunoprecipitated, only TSG101, but not HRS or ALIX, was detected in the IP suggesting a potential direct interaction between CPAP and TSG101. Interestingly, EGF treatment to stimulate EVT of EGFR caused a profound increase in the amount of TSG101 bound to CPAP compared to unstimulated cells, albeit the amounts of GFP-CPAP in the IP were not considerably different, suggesting a possible interaction between CPAP and oligomerized TSG101. In fact, a previous report has shown that coiled-coil domain of TSG101 contributes to its homo-tetramerization (*51*). Our observations that post-EGF-treatment, TSG101 pulldown by HRS and HRS pulldown by TSG101, are diminished under CPAP deficiency suggests that CPAP may be critical for a stable interaction between HRS and TSG101 during vesicular transport of receptor cargo. Previous reports (*18, 52*) have shown that TSG101 depletion inhibits MVB formation and alters the morphology of the early endosome in unstimulated cells, and more profoundly in EGF stimulated cells suggesting that TSG101 is required for the formation of stable vacuolar domains within the early endosome that develop into MVBs. In this regard, our previous report on the diminished ILV budding/MVB formation and EGFR degradation under CPAP deficiency (*25*) and the current observations on CPAP-TSG101-HRS interaction dynamics propose the hypothesis that CPAP-TSG101 interaction is essential for the ESCRT function pertinent to MVB biogenesis during the vesicular transport of receptor cargo.

An important question of how the functional interaction between CPAP and ESCRT protein influences the Rab5-to-Rab7 conversion remains unanswered by our studies. A study employing yeast model has shown that ESCRT disruption inhibits the completion of Rab5-to-Rab7 conversion, but disruption of Rabs impedes ESCRT function, at endosomes as well (*34*) . Another study showed that ESCRTs function upstream of Rab conversion and loss of early ESCRTs leads to inhibition of Rab conversion (*35*). Nevertheless, co-ordination between ESCRT and Rab conversion and the associated molecular events during the vesicular transport are largely unknown. Our previous report (*25*) and current study together show that depletion of CPAP function disrupts TSG101 (ESCRT-I) function, MVB formation and Rab conversion during EVT of EGFR. Consistent with TSG101 recruitment to endosomes, overexpression of ESCRT-0 protein HRS, but not TSG101 itself, caused effective restoration of Rab5-Rab7 conversion and EVT of ligand bound EGFR to MVBs in CPAP depleted cells. Our observations are consistent with the above-mentioned reports (*34, 35*) that suggest ESCRT functions upstream of Rab5-to-Rab7 conversion and CPAP may play a crucial role to bridge the two processes.

In conclusion, we establish a previously unknown, non-centrosomal localization property and endosome-associated function for a centriole biogenesis protein, CPAP. We show that CPAP facilitate ESCRT function and MVB biogenesis, Rab5-to-Rab7 conversion, and endosome maturation by recruiting an ESCRT-I member TSG101 to the early endosome during MVB formation. We also demonstrate, for the first time, a functional interaction between CPAP and an ESCRT protein which is critical for bridging ESCRT-0 and ESCRT-I functions during the early events of MVB formation. Several centrosome-associated canonical cellular processes including centriole duplication, spindle orientation and positioning, and ciliogenesis have been attributed to CPAP before (*22, 24, 26, 28, 29, 53*). Our recent reports have shown that CPAP has a role in positively regulating EVT of ligand bound EGFR to lysosome for degradation to prevent persistent signaling by this receptor (*25*). However, a role of CPAP in regulating ESCRT function and endosome maturation has never been described before. Importantly, whether this newly identified, non-canonical function of CPAP in regulating ESCRT function and endosome maturation is required for the above-mentioned well-recognized canonical functions, or if they operate independently remains to be studied. Further studies are also required to establish if CPAP functions as a “bonafide” ESCRT component or a critical ESCRT associated protein and how it is involved in various other ESCRT dependent cellular functions. Nevertheless, our novel

observations described here will open a new area of studies to determine if and how the fundamental cellular processes such as centriole duplication and endosomal transport of cargo proteins are coupled. Our observations on a critical role for CPAP in facilitating ESCRT function could also help to better explain the potential molecular mechanisms of CPAP mutation associated diseases such as microcephaly.

Conflict of Interest statement: Authors do not have any conflict(s) of interest to disclose.

Author contribution: R. G. conceived the idea, designed experiments, researched and analyzed data, and wrote/edited the manuscript, and C.V. designed experiments and wrote/edited the manuscript.

Footnote: This work was supported by National Institutes of Health (NIH) grant R01DE030331 and R21DE026965 to C.V. and R.G. Unrestricted research funds from Holling Cancer Center and College of Medicine, MUSC supported some aspects of the study. As the corresponding author, Dr. Gudi is the guarantor of this work and as such, has full access to all the data in the study and takes responsibility for integrity of the data and accuracy of data analysis. The authors are thankful to the Electron microscopy core and the Cell & Molecular Imaging Shared Resource which is supported by the Hollings Cancer Center, Medical University of South Carolina (P30 CA138313) and the Shared Instrumentation Grant S10 OD018113 as well as the flow cytometry core of MUSC for the FACS instrumentation support.

Abbreviations:

ESCRT, Endosomal sorting complex for recruitment and transport; **TSG101**, Tumor susceptibility gene 101; **HRS**, Hepatocyte growth factor-regulated tyrosine kinase substrate, **EGF**, Epidermal growth factor; **EGFR**, Epidermal growth factor receptor, **MVB**, Multivesicular bodies; **ILV**, Intraluminal vesicle; **EVT** Endocytic vesicular transport.

Figure legends:

Fig. 1. CPAP-depletion does not affect Rab5 recruitment to endosomes and ligand-bound EGFR positive vesicular structures. HeLa cells expressing control or CPAP shRNA were treated with AF555-EGF ligand for indicated time points and stained for Rab5 and EEA1 **(A)**, Rab5 and CD63 **(B)**, or Rab5 (along with AF555-EGF) and imaged by confocal microscopy **(C)**. Left panels (A-C): maximum intensity-projection images of confocal Z stacks. Right panels (A-C): Single Z-plane of images. Bottom left graph in C; percentages of EGF-positive (red) puncta showing Rab5 (green) colocalization (yellow) quantified in single Z-planes of multiple cells across at least 3 experiments. Bottom right graph in C; Relative integrated fluorescence intensity values of Rab5 staining quantified in single Z-planes of multiple cells across at least 3 experiments. Scale bar: 10µm. *p*-values were not statistically significant.

Fig. 2. CPAP-depletion disrupts Rab7 recruitment to endosomes and ligand-bound EGFR positive vesicular structures. HeLa cells expressing control or CPAP shRNA were treated with AF555-EGF ligand for indicated time points and stained for Rab7 and EEA1 **(A)**, Rab7 and CD63 **(B)**, or Rab7 (along with AF555-EGF) and imaged by confocal microscopy **(C)**. Left panels (A-C): maximum intensity-projection images of confocal Z stacks. Right panels (A-C): Single Z-plane of images. Bottom left graph in C; percentages of EGF-positive (red) puncta showing Rab7 (green) colocalization (yellow) quantified in single Z-planes of multiple cells across at least 3 experiments. Bottom right graph in C; Relative integrated fluorescence intensity values of Rab7 staining quantified in single Z-planes of multiple cells across at least 3 experiments are shown. Scale bar: 10µm. *p*-values: *<0.05, ****<0.0001

Fig. 3. CPAP depletion disrupts Rab5-to-Rab7 conversion. A) HeLa cells expressing control or CPAP shRNA were treated with untagged EGF for 60min, stained for Rab5 and Rab7, and imaged by Airyscan super-resolution microscopy. Left panel: maximum intensity-projection images of Z stacks; middle panel: single Z-plane of images; right panel: percentages of Rab5-positive (green) puncta showing Rab7 (red) colocalization (yellow) quantified in single Z-planes of multiple cells across at least 3 experiments. **B)** HeLa cells stably expressing control or CPAP-shRNA were transfected with control vector (GFP), or GFP-Rab7 (WT; wild-type) or GFP-Rab7 (DN; dominant negative) vector constructs, treated with AF555-EGF ligand for 60min, and stained for CD63 to mark MVBs/late endosomes, and imaged by confocal microscopy to determine

AF555-EGF and CD63 colocalization. Left top row: GFP expression in control and Rab7 construct expressing cells; left lower rows: representative single Z-plane of images showing ligand-bound EGFR-CD63 colocalization; right panel: percentages of CD63-positive (green; pseudo color) puncta showing AF555-EGF (red) colocalization (yellow) quantified in single Z-planes of multiple cells across at least 3 experiments. Scale bar: 10µm. *p*-values: ****<0.0001.

Fig. 4. Recruitment of TSG101 to the endosomes is compromised in CPAP depleted cells. HeLa cells expressing control or CPAP shRNA were treated with untagged EGF for 60min, stained for ESCRT pathway proteins HRS, TSG101 or ALIX along with EEA1 (to mark early endosome), and imaged by Airyscan super-resolution microscopy. Left panels: representative single Z-plane of images showing localization of HRS, TSG101, or ALIX on EEA1 positive puncta. Right panels: percentages of EEA1 (green) puncta showing ESCRT protein (red) colocalization (yellow) quantified in single Z-planes of multiple cells across at least 3 experiments. Scale bar: 10µm. *p*-values: ****<0.0001.

Fig. 5. CPAP is detected on endosomes in quiescent and EGF treated cells and it colocalizes with ESCRT proteins. **A)** HeLa cells were treated with untagged EGF for different time-points, stained for EEA1 and CPAP, and imaged by Lightning super-resolution microscopy. Left panel: single Z-plane of images showing EEA1 and CPAP staining of representative cells; right panel: percentages of EEA1-positive (green) puncta showing CPAP (red) colocalization (yellow) quantified in single Z-planes of multiple cells across at least 3 experiments. **B)** HeLa cells treated with untagged EGF for indicated time points, were stained with AF488 linked sheep anti-EEA antibody, rabbit anti-CPAP, and mouse anti-HRS or -TSG101 primary antibodies followed by AF647 and AF568 linked anti-rabbit and anti-mouse secondary antibodies and imaged using Lightning super-resolution microscopy. Left panel: representative single Z-plane of images showing colocalization of CPAP along with HRS or TSG101 on EEA1 positive puncta. Right panels: Colocalization of CPAP (red) and HRS or TSG101 (magenta) on EEA1 (green) positive puncta was quantified in single Z-planes of multiple cells across at least 3 experiments. Scale bar: 10µm. *p*-values: *<0.05, ** <0.01, ***,0.001, ****<0.0001. **C)** HEK293T cells stably expressing doxycycline inducible GFP-CPAP were subjected to endosome fractionation by ultracentrifugation approach. Endosome fraction and whole cell lysates as input control were probed for indicated proteins by IB. **D)** HEK293T cells left untreated or treated with untagged

EGF for different time points were subjected to endosome fractionation, and the endosome fractions and whole cell lysate were subjected to IB for indicated protein.

Fig. 6. Exogenous expression of CPAP restores TSG101 recruitment on to early endosomes in CPAP and HRS depleted cells. A) Schematic depiction of experimental strategy using control, CPAP and HRS specific siRNA treated HeLa cells with and without siRNA-resistant GFP-CPAP expression. **B)** Airyscan super resolution microscopy images showing cells stained for EEA1 and TSG101. Left panel: representative single Z-plane of images showing localization of TSG101 on EEA1 positive puncta in cells with and without GFP-CPAP expression. Right panel: percentages of EEA1 (green, pseudo-color) puncta showing TSG101 (red) colocalization (yellow) quantified in single Z-planes of multiple cells across at least 3 experiments. Scale bar: 10µm. *p*-values: ** <0.01, ***,0.001, ****<0.0001.

Fig. 7. HRS overexpression restored TSG101 recruitment onto endosome and EVT function in CPAP-depleted cells. A) Schematic depiction of experimental strategy using control and CPAP specific siRNA treated HeLa cells with and without GFP-HRS or GFP-TSG101 expression. **B)** Lightning super resolution microscopy images showing cells stained for EEA1 and TSG101. Left panel: representative single Z-plane of images showing localization of TSG101 on EEA1 positive puncta in cells with and without GFP-HRS or GFP-TSG101 expression. Right panel: percentages of EEA1 (green, pseudo-color) puncta showing TSG101 (red) colocalization (yellow) quantified in single Z-planes of multiple cells across at least 3 experiments. **C)** Cells treated with AF555 linked EGF were stained for CD63 and imaged as done for panel B. Left panel: representative single Z-plane of images showing localization of AF555-EGF on CD63 positive puncta in cells with and without GFP-HRS or GFP-TSG101 expression. Right panel: percentages of CD63 (green, pseudo-color) puncta showing EGF (red) colocalization (yellow) quantified in single Z-planes of multiple cells across at least 3 experiments. Scale bar: 10µm. *p*-values: *<0.05, ** <0.01, ****<0.0001.

Fig. 8. CPAP depletion does not impact cellular levels of TSG101 and other ESCRT proteins. HeLa and HEK293T cells were treated with control or CPAP specific siRNA for 48h and subjected to IB to detect the cellular levels of CPAP and ESCRT proteins **(A&C)**. Cells were also subjected to intracellular staining and flow cytometry to detect cellular levels of CPAP and TSG101**(B&D)**. Representative IB images of three independent experiments that produced similar trend in

outcomes are shown for panels A&C. Representative histogram overlay plots (left) and mean fluorescence intensity (MFI) values of three independent experiments (right) are shown for panels B&D.

Fig. 9. CPAP interacts with ESCRT proteins. A) CPAP is detected in IP of ESCRT protein specific IPs. Lysates of HeLa cells were subjected to IP using control antibody or anti -HRS, -TSG101- or -ALIX antibodies followed by IB using indicated antibodies. **B) CPAP-TSG101 interaction is enhanced upon EGF treatment.** Doxycycline-inducible GFP-CPAP expressing HEK293T cells were treated with doxycycline for 24h, left untreated or treated with EGF ligand for 45min, and subjected to IP using anti-GFP antibody and IB using indicated ESCRT protein specific antibodies. **C&D) Interaction between HRS and TSG101 is abrogated in CPAP-deficient cells.** HeLa cells were treated with control and CPAP specific siRNA for 48h, and EGF for 45min and subjected to IP using control antibody or anti-TSG101 (C) or -HRS (D) antibodies, followed by IB using TSG101 and HRS specific antibodies. All results are representative of at least three experiments that produced similar trend in outcomes.

Fig. 10. Rab5-to-Rab7 conversion and EGFR trafficking to late endosome are restored in CPAP-depleted cells upon HRS, but not TSG101, overexpression. Control and CPAP specific siRNA treated HeLa cells were subjected to mock or GFP-HRS or GFP-TSG101 vector transfection for 24h, treated with untagged EGF for 60min and stained for Rab5 and Rab7 **(A)** or treated with AF555-EGF for 60min and stained for Rab7 **(B)** and imaged by Lightning super resolution microscopy. Left panels: representative single Z-plane of images showing localization of Rab7 on Rab5 positive puncta (A) and AF555-EGF on Rab7 positive puncta (B) in cells with and without GFP-HRS or GFP-TSG101 expression. Right panels: percentages of Rab5 (green, pseudo-color) puncta showing Rab7 (red) colocalization (yellow) (A) or Rab7 (green, pseudo-color) puncta showing AF555-EGF (red) colocalization (yellow) (B) quantified in single Z-planes of multiple cells across at least 3 experiments. Scale bar: 10µm. *p*-values: *<0.05, ** <0.01, ****<0.0001.

Supplemental Fig. 1: Cellular levels of Rab5 and Rab7 are not impacted by CPAP depletion. Immunoblotting of control and CPAP shRNA-expressing HeLa cell lysates was performed with Rabbit anti-CPAP antibody, and anti-Rab5 and anti-Rab7 antibodies.

Supplemental Fig. 2: Validating CPAP-specific antibody. HEK293T and HeLa cell lysates expressing control or CPAP siRNA were immunoblotted with mouse anti-CPAP antibody.

Supplemental Fig. 3: Rab5-to-Rab7 conversion is hampered in CPAP siRNA treated cells. Using Airyscan super-resolution, co-localization between Rab5 and Rab7 at 60m of EGF ligand treatment was performed using control and CPAP siRNA treated HeLa cells. Scale bar: 10µm.

Supplemental Fig. 4: CPAP was not found in Rab5 and Rab7 specific IPs. HEK293T cells transfected with GFP or GFP-Rab7 and GFP-Rab5 expression vectors were subjected to immunoprecipitation with the anti-GFP antibody. Immunoblotting was performed as indicated.

Supplemental Fig. 5: V**alidating ESCRT protein specific antibodies. C**ontrol or anti-HRS, -TSG101, and -ALIX specific siRNA treated HeLa cells were tested for knockdown efficiency by immunoblotting (left panels) as well as by Airyscan super-resolution microscopy (right panels). Right panel shows single Z images of representative cells.

Supplemental Fig. 6: HRS depletion limits TSG101 recruitment to the early endosomes during EVT. Control or HRS-siRNA treated HeLa cells were exposed to EGF for 60m and stained using anti-EEA1 and -TSG101 antibodies. Images were acquired using Airyscan super-resolution. Scale bar: 10µm. $p<0.0001$.

Supplemental Fig. 7: CPAP is detected on early endosomes in quiescent and EGF-treated cells. Control or CPAP-siRNA treated HeLa cells were left untreated or treated with EGF for 45min, followed by staining with rabbit anti-CPAP and -mouse anti-EEA1 antibodies. Images were acquired using Lightning super-resolution microscope. Scale bar: 10µm.

Supplemental Fig. 8: CPAP expression is observed on endosomes by TEM. HeLa cells treated with EGF for 60min were subjected to transmission electron microscopy (TEM)-immunogold analysis. 70nm thin sections on gold grids were stained with rabbit anti-CPAP antibody alone **(A)**

or along with -mouse anti-EEA1 antibody **(B)**, and anti-rabbit-IgG-gold (15nm) and anti-mouse IgG-gold (6nm) conjugates.

Supplemental Fig. 9: Cellular levels of ESCRT proteins are unchanged upon EGF treatment. Control or CPAP siRNA treated HEK293T cells were treated with EGF for 60min and subjected to immunoblotting with indicated ESCRT protein specific antibodies and anti-CPAP antibody.

Materials and Methods:

Cell lines: HEK293T and HeLa cells were used in this study. These cells were cultured in DMEM media, supplemented with 10% FBS, HEPES, sodium pyruvate, sodium bicarbonate and minimum essential amino acids.

Reagents: Transfection of HEK293T and HeLa cells using plasmids was done using calcium-phosphate method and Trans-X2 reagent (Mirus) respectively. Transfection of siRNA in both cell types was done by using the Trans-siQuest (Mirus). siRNA/shRNA regions targeted in CPAP have been described previously(*25*). RNAi resistant GFP-CPAP overexpression construct was kindly provided by Dr. Pierre Gonczy (EPFL, Lausanne). Constructs expressing GFP-HRS and GFP-TSG101 were kindly provided by Dr. Clarisse Berlioz-Torrent (Institut Cochin, Paris). siRNA against HRS, ALIX and TSG101 were purchased from Santa Cruz Biotech. Primary antibodies used in this study: rabbit anti-CPAP (Proteintech,11517-1-AP); mouse anti-CPAP(Abnova, H00055835-M01); anti-Rab5 (Proteintech, 20228-1-AP); anti-Rab7 (Proteintech, 55469-1-AP or Santa Cruz, sc-376362; -Actin (Proteintech, 60008-1-Ig); -GFP (Proteintech, 66002-1-Ig or 50430-2-AP); -HRS (Santa Cruz, sc-271455); -TSG101 (Santa Cruz, sc-7964 ; Proteintech, 28283-1-AP); and -ALIX (Biolegend, 634502), EEA1 (Invitrogen, PA1-0337 or BD biosciences 610456) and CD63 (BD biosciences, 556019). Alexa fluor 555 (AF555)- tagged EGF and untagged EGF were purchased from Invitrogen and Tonbo biosciences respectively.

Immunofluorescence: Cells were grown on sterile coverslips in a 24-well plate. After appropriate experimental treatments, cells were fixed with 4% paraformaldehyde. Permeabilization was done using 0.1% saponin containing buffer for 30min at RT. Post-blocking with 1% BSA, primary and secondary antibody incubations were done at 37ºC for 2h and 1h respectively. Coverslips were mounted using Prolong gold antifade mounting reagent (Invitrogen) and imaged using Zeiss 880 confocal or Airyscan or Leica Stellaris or Lightning super-resolution unit, using the 63X oil immersion objective with n.a. 1.4, as indicated. Optimal recommended settings were used to acquire Z stacks.

Image quantification and statistical considerations.

Prior to image analysis, Airyscan files were automatically processed using the Zen software (version 2.0) of Zeiss (https:// www. zeiss. com/ micro scopy/us/ produ cts/ micro scope- softw are/ zen. html). Leica Lightning images were also obtained as processed and deconvolution-based

images that were ready to be analyzed. Images are presented as maximum intensity projection, or a single Z plane as indicated. Z-stack images were split into single Z planes and, for example: green (in most cases, EEA1 positive endosomes) and yellow pixels were quantified to determine the percentage of colocalization as indicated in the experiment. Quantification of colocalization was done manually in the single Z scans. Single Z-plane of each cell area that showed maximum number of endocytic vesicular structures were considered for quantification and image presentation. In EGF trafficking experiments, total number of red (AF555-EGF) and red puncta localized to green puncta (yellow; EGF + endosome marker) were counted per cell area from multiple experiments using the multi-point tool and counter of ImageJ software version 1.53 (https:// imagej. nih. gov/ ij/) for determining percentage colocalization. Total fluorescence intensity of immunofluorescent cells was determined by calculating the integrated density using ImageJ software. Experiments were repeated several times and all figure panels presented here represent at least three experiments that produced similar trend in outcomes. Cumulative values or values from a representative experiment were used for graphical presentation of data to indicate trend. *P*-values were calculated using GraphPad Prism statistical analysis software version 10 (https:// www. graph pad. com/ scien tific- softw are/ prism/).

Western blotting: Cells harvested at different time-points were lysed using RIPA buffer supplemented with 0.1M PMSF and protease inhibitor cocktail. Lysates were then spun at 14000 rpm for 30min at 4°C, supernatants were separated, and boiled at 95°C for 10m after addition of SDS sample buffer. Post-SDS-PAGE and Western blotting, immublotted PVDF membranes were developed using SuperSignal West Dura substrate (Thermo Scientific) Chemiluminescence substrate and ChemiDoc imager (Biorad). Anti-rabbit-IgG HRP and -mouse-IgG HRP were obtained from Amersham and Biorad respectively.

Transmission electron microscopy: HeLa cells treated with EGF ligand for 60min were fixed using 1% glutaraldehye, dehydrated and embedded in LR white resin (Ted Pella, Inc). 70nm thin sections on gold grids were blocked with blocking buffer (20mM Hepes, 1% fish gelation and 0.4% Triton X-100) at RT for 1h and incubated with rabbit anti-CPAP (Proteintech) or with mouse anti-EEA1 (BD biosciences) antibodies overnight at 4ºC, followed by incubation with anti-rabbit IgG conjugated with 15nm gold particles or anti-mouse IgG linked to 6nm gold particles (Ted

Pella, Inc) for 1h at RT. After extensive washing, sections were further stained with 1% Uranyl acetate for contrast and analyzed using JEOL1210 transmission electron microscope.

Endosome fractionation: Cell pellets were rinsed twice with cold PBS and treated with 300 µl homogenization buffer (3mM imidazole, pH 7.4, 250 mM sucrose, 0.5 mM EDTA and protease inhibitors. Cells were homogenized with 20 strokes of a tight fitting Dounce homogenizer and centrifuged for 10 min at 3000 rpm in a tabletop centrifuge. The resulting post nuclear supernatant was adjusted to 40.6% sucrose using 62% sucrose. Diluted supernatant was placed in mini centrifuge tubes and overlayed with 700 µl of 35% and 500 µl of 25% sucrose solutions, followed by ultracentrifugation at 108,000g for 3h at 4ºC. The endosome enriched fraction at the 25/35% interface was collected, diluted threefold with cold PBS and centrifuged at 108,000g for 30 mins. Pellets were treated with SDS sample buffer and subjected to immunoblotting.

Flow cytometry: Cells were fixed with 4% PFA for 15mins at RT, followed by rinse with 1X permeabilization buffer (PB) containing 0.1% saponin. Cells were then incubated with PBS for 30 mins at RT, blocked with 1% donkey serum in PB, incubated with primary antibodies for 2h at 37ºC and fluorochrome labeled secondary antibodies for 1h at 37ºC. Cells were acquired using FACS Verse instrument and analyzed using the Flowjo software.

References:

1. C. C. Scott, F. Vacca, J. Gruenberg, Endosome maturation, transport and functions. *Semin Cell Dev Biol* **31**, 2-10 (2014).
2. S. L. Schmid, A. Sorkin, M. Zerial, Endocytosis: Past, present, and future. *Cold Spring Harb Perspect Biol* **6**, a022509 (2014).
3. A. V. Vieira, C. Lamaze, S. L. Schmid, Control of EGF receptor signaling by clathrin-mediated endocytosis. *Science* **274**, 2086-2089 (1996).
4. M. Mettlen, P. H. Chen, S. Srinivasan, G. Danuser, S. L. Schmid, Regulation of Clathrin-Mediated Endocytosis. *Annual review of biochemistry* **87**, 871-896 (2018).
5. H. Neto, L. L. Collins, G. W. Gould, Vesicle trafficking and membrane remodelling in cytokinesis. *Biochem J* **437**, 13-24 (2011).
6. I. Mellman, W. J. Nelson, Coordinated protein sorting, targeting and distribution in polarized cells. *Nat Rev Mol Cell Biol* **9**, 833-845 (2008).
7. R. Villasenor, Y. Kalaidzidis, M. Zerial, Signal processing by the endosomal system. *Curr Opin Cell Biol* **39**, 53-60 (2016).
8. A. Tomas, C. E. Futter, E. R. Eden, EGF receptor trafficking: consequences for signaling and cancer. *Trends Cell Biol* **24**, 26-34 (2014).
9. C. E. Futter, A. Pearse, L. J. Hewlett, C. R. Hopkins, Multivesicular endosomes containing internalized EGF-EGF receptor complexes mature and then fuse directly with lysosomes. *J Cell Biol* **132**, 1011-1023 (1996).
10. R. C. Piper, D. J. Katzmann, Biogenesis and function of multivesicular bodies. *Annu Rev Cell Dev Biol* **23**, 519-547 (2007).
11. J. Gruenberg, H. Stenmark, The biogenesis of multivesicular endosomes. *Nat Rev Mol Cell Biol* **5**, 317-323 (2004).
12. M. Zerial, Regulation of endocytosis by the small GTP-ase rab5. *Cytotechnology* **11 Suppl 1**, S47-49 (1993).
13. H. Stenmark, Rab GTPases as coordinators of vesicle traffic. *Nature reviews. Molecular cell biology* **10**, 513-525 (2009).
14. M. A. Barbieri *et al.*, Epidermal growth factor and membrane trafficking. EGF receptor activation of endocytosis requires Rab5a. *The Journal of cell biology* **151**, 539-550 (2000).
15. J. Rink, E. Ghigo, Y. Kalaidzidis, M. Zerial, Rab conversion as a mechanism of progression from early to late endosomes. *Cell* **122**, 735-749 (2005).
16. D. Poteryaev, S. Datta, K. Ackema, M. Zerial, A. Spang, Identification of the switch in early-to-late endosome transition. *Cell* **141**, 497-508 (2010).
17. Q. Lu, L. W. Hope, M. Brasch, C. Reinhard, S. N. Cohen, TSG101 interaction with HRS mediates endosomal trafficking and receptor down-regulation. *Proc Natl Acad Sci U S A* **100**, 7626-7631 (2003).
18. M. Razi, C. E. Futter, Distinct roles for Tsg101 and Hrs in multivesicular body formation and inward vesiculation. *Mol Biol Cell* **17**, 3469-3483 (2006).
19. K. G. Bache, A. Brech, A. Mehlum, H. Stenmark, Hrs regulates multivesicular body formation via ESCRT recruitment to endosomes. *J Cell Biol* **162**, 435-442 (2003).
20. W. M. Henne, N. J. Buchkovich, S. D. Emr, The ESCRT pathway. *Dev Cell* **21**, 77-91 (2011).

21. J. H. Cho, C. J. Chang, C. Y. Chen, T. K. Tang, Depletion of CPAP by RNAi disrupts centrosome integrity and induces multipolar spindles. *Biochem Biophys Res Commun* **339**, 742-747 (2006).
22. L. Y. Hung, C. J. Tang, T. K. Tang, Protein 4.1 R-135 interacts with a novel centrosomal protein (CPAP) which is associated with the gamma-tubulin complex. *Mol Cell Biol* **20**, 7813-7825 (2000).
23. L. Y. Hung, H. L. Chen, C. W. Chang, B. R. Li, T. K. Tang, Identification of a novel microtubule-destabilizing motif in CPAP that binds to tubulin heterodimers and inhibits microtubule assembly. *Mol Biol Cell* **15**, 2697-2706 (2004).
24. C. J. Tang, R. H. Fu, K. S. Wu, W. B. Hsu, T. K. Tang, CPAP is a cell-cycle regulated protein that controls centriole length. *Nat Cell Biol* **11**, 825-831 (2009).
25. R. Gudi, V. Palanisamy, C. Vasu, Centrosomal P4.1-associated protein (CPAP) positively regulates endocytic vesicular transport and lysosome targeting of EGFR. *Sci Rep* **11**, 12689 (2021).
26. G. Kohlmaier *et al.*, Overly long centrioles and defective cell division upon excess of the SAS-4-related protein CPAP. *Curr Biol* **19**, 1012-1018 (2009).
27. T. I. Schmidt *et al.*, Control of centriole length by CPAP and CP110. *Curr Biol* **19**, 1005-1011 (2009).
28. K. S. Wu, T. K. Tang, CPAP is required for cilia formation in neuronal cells. *Biol Open* **1**, 559-565 (2012).
29. X. Zheng *et al.*, Molecular basis for CPAP-tubulin interaction in controlling centriolar and ciliary length. *Nat Commun* **7**, 11874 (2016).
30. E. Gabriel *et al.*, CPAP promotes timely cilium disassembly to maintain neural progenitor pool. *EMBO J* **35**, 803-819 (2016).
31. A. Sharma *et al.*, Centriolar CPAP/SAS-4 Imparts Slow Processive Microtubule Growth. *Dev Cell* **37**, 362-376 (2016).
32. R. R. Gudi, H. Janakiraman, P. H. Howe, V. Palanisamy, C. Vasu, Loss of CPAP causes sustained EGFR signaling and epithelial-mesenchymal transition in oral cancer. *Oncotarget* **12**, 807-822 (2021).
33. M. Babst, MVB vesicle formation: ESCRT-dependent, ESCRT-independent and everything in between. *Curr Opin Cell Biol* **23**, 452-457 (2011).
34. M. R. Russell, T. Shideler, D. P. Nickerson, M. West, G. Odorizzi, Class E compartments form in response to ESCRT dysfunction in yeast due to hyperactivity of the Vps21 Rab GTPase. *J Cell Sci* **125**, 5208-5220 (2012).
35. D. P. Ott, S. Desai, J. A. Solinger, A. Kaech, A. Spang, Coordination between ESCRT function and Rab conversion during endosome maturation. *EMBO J* **44**, 1574-1607 (2025).
36. O. Pornillos *et al.*, HIV Gag mimics the Tsg101-recruiting activity of the human Hrs protein. *J Cell Biol* **162**, 425-434 (2003).
37. P. G. Woodman, C. E. Futter, Multivesicular bodies: co-ordinated progression to maturity. *Curr Opin Cell Biol* **20**, 408-414 (2008).
38. J. Kleylein-Sohn *et al.*, Plk4-induced centriole biogenesis in human cells. *Dev Cell* **13**, 190-202 (2007).
39. R. Vitelli *et al.*, Role of the small GTPase Rab7 in the late endocytic pathway. *J Biol Chem* **272**, 4391-4397 (1997).

40. B. P. Ceresa, S. J. Bahr, rab7 activity affects epidermal growth factor:epidermal growth factor receptor degradation by regulating endocytic trafficking from the late endosome. *J Biol Chem* **281**, 1099-1106 (2006).
41. S. B. Shields, R. C. Piper, How ubiquitin functions with ESCRTs. *Traffic* **12**, 1306-1317 (2011).
42. B. Korbei, Ubiquitination of the ubiquitin-binding machinery: how early ESCRT components are controlled. *Essays Biochem* **66**, 169-177 (2022).
43. C. Raiborg, K. G. Bache, A. Mehlum, E. Stang, H. Stenmark, Hrs recruits clathrin to early endosomes. *EMBO J* **20**, 5008-5021 (2001).
44. M. R. Dores *et al.*, AP-3 regulates PAR1 ubiquitin-independent MVB/lysosomal sorting via an ALIX-mediated pathway. *Mol Biol Cell* **23**, 3612-3623 (2012).
45. C. Bissig, J. Gruenberg, ALIX and the multivesicular endosome: ALIX in Wonderland. *Trends Cell Biol* **24**, 19-25 (2014).
46. E. B. Frankel, A. Audhya, ESCRT-dependent cargo sorting at multivesicular endosomes. *Semin Cell Dev Biol* **74**, 4-10 (2018).
47. J. R. Mayers, A. Audhya, Vesicle formation within endosomes: An ESCRT marks the spot. *Commun Integr Biol* **5**, 50-56 (2012).
48. T. Slagsvold, K. Pattni, L. Malerod, H. Stenmark, Endosomal and non-endosomal functions of ESCRT proteins. *Trends Cell Biol* **16**, 317-326 (2006).
49. W. I. Sundquist *et al.*, Ubiquitin recognition by the human TSG101 protein. *Mol Cell* **13**, 783-789 (2004).
50. E. Morita *et al.*, Human ESCRT and ALIX proteins interact with proteins of the midbody and function in cytokinesis. *EMBO J* **26**, 4215-4227 (2007).
51. J. T. White, D. Toptygin, R. Cohen, N. Murphy, V. J. Hilser, Structural Stability of the Coiled-Coil Domain of Tumor Susceptibility Gene (TSG)-101. *Biochemistry* **56**, 4646-4655 (2017).
52. A. Doyotte, M. R. Russell, C. R. Hopkins, P. G. Woodman, Depletion of TSG101 forms a mammalian "Class E" compartment: a multicisternal early endosome with multiple sorting defects. *J Cell Sci* **118**, 3003-3017 (2005).
53. D. Kitagawa *et al.*, Spindle positioning in human cells relies on proper centriole formation and on the microcephaly proteins CPAP and STIL. *J Cell Sci* **124**, 3884-3893 (2011).

Fig. 1

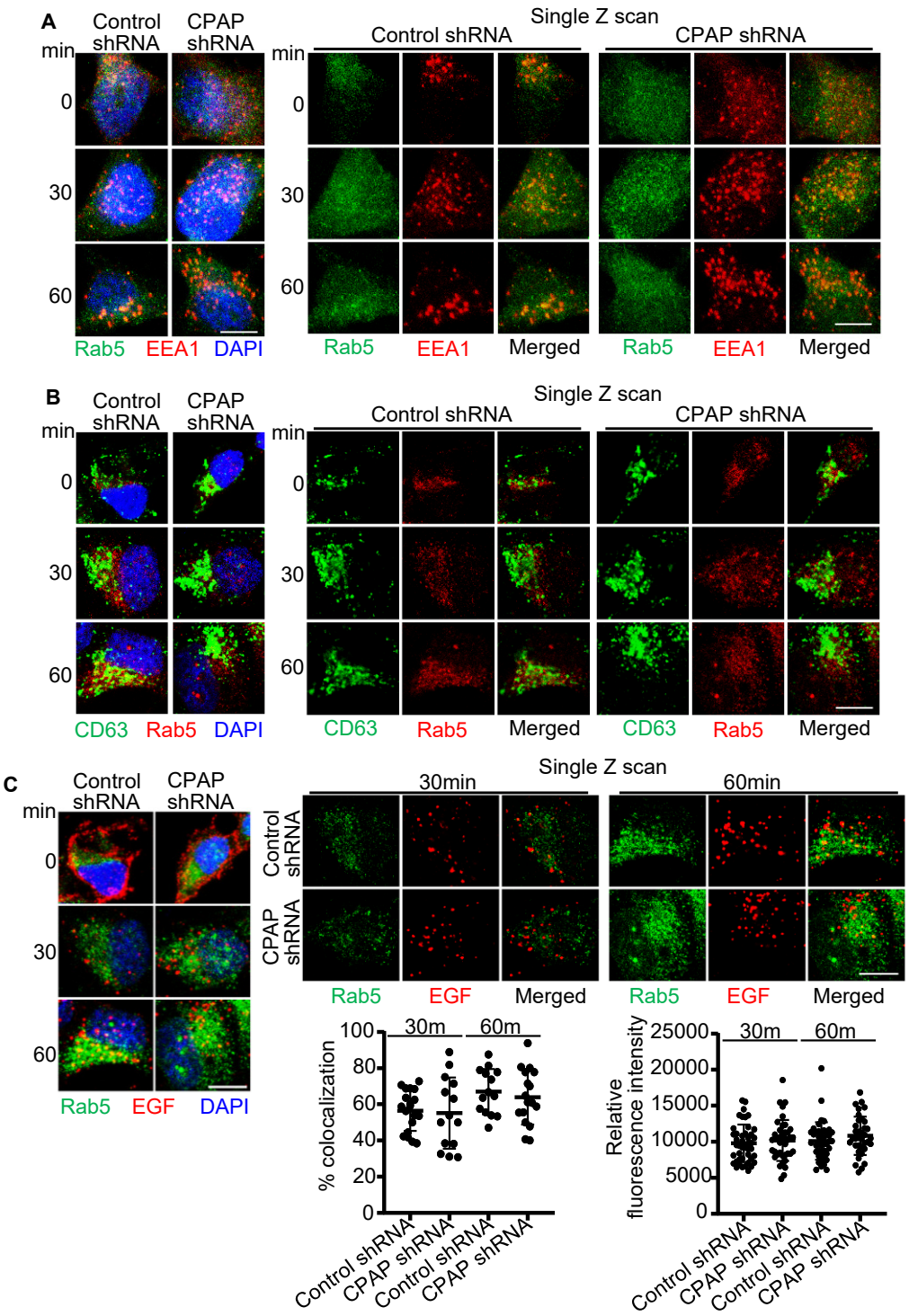
A
Control shRNA
CPAP shRNA
min
0
30
60
Rab5 EEA1 DAPI
Single Z scan
Control shRNA
CPAP shRNA
Rab5 EEA1 Merged
B
CD63 Rab5 DAPI
CD63 Rab5 Merged
C
Rab5 EGF DAPI
30min
60min
Control shRNA
CPAP shRNA
Rab5 EGF Merged
% colocalization
30m
60m
Relative fluorescence intensity

Fig. 2

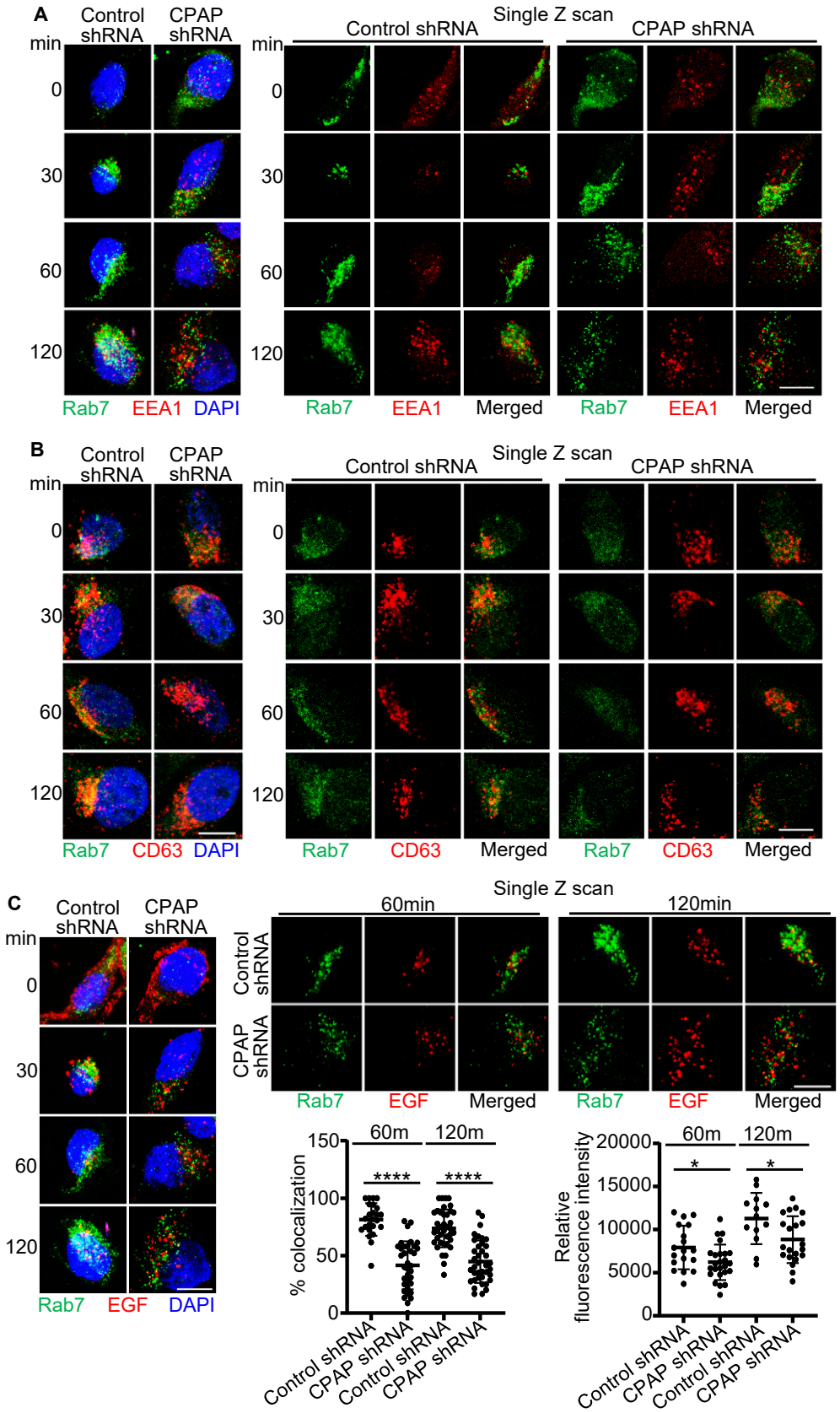
A
Control shRNA
CPAP shRNA
min
0
30
60
120
Rab7 EEA1 DAPI
Single Z scan
Control shRNA
CPAP shRNA
Rab7 EEA1 Merged
B
Rab7 CD63 DAPI
Rab7 CD63 Merged
C
Rab7 EGF DAPI
60min
120min
Control shRNA
CPAP shRNA
Rab7 EGF Merged
% colocalization
Relative fluorescence intensity
60m
120m
****
*
Control shRNA
CPAP shRNA

Fig. 3

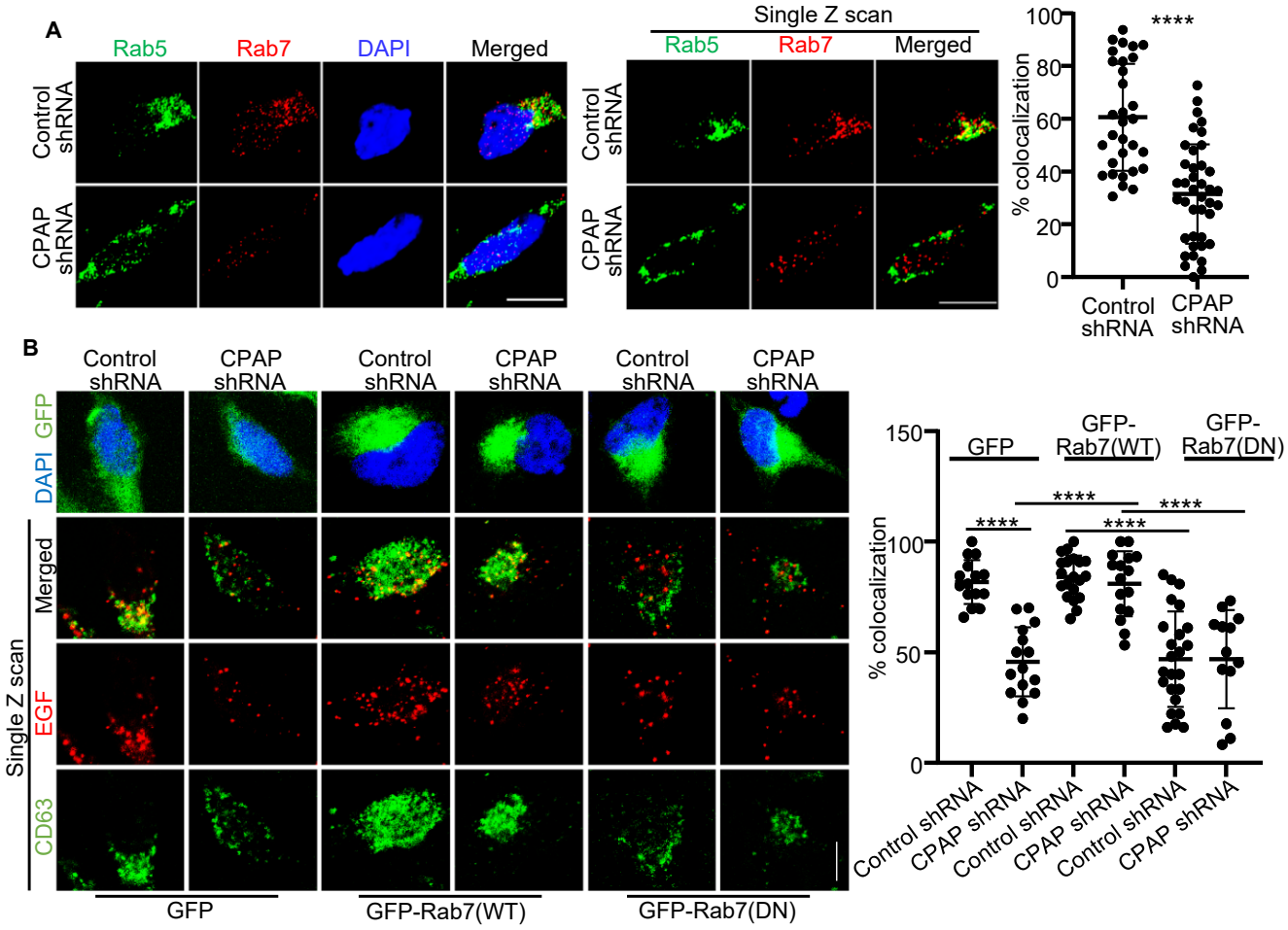
A
Rab5
Rab7
DAPI
Merged
Control shRNA
CPAP shRNA
Single Z scan
Rab5
Rab7
Merged
Control shRNA
CPAP shRNA
% colocalization
100
80
60
40
20
0
****
Control shRNA
CPAP shRNA
B
Control shRNA
CPAP shRNA
Control shRNA
CPAP shRNA
Control shRNA
CPAP shRNA
GFP
DAPI
Merged
EGF
CD63
Single Z scan
GFP
GFP-Rab7(WT)
GFP-Rab7(DN)
% colocalization
150
100
50
0
GFP
GFP-Rab7(WT)
GFP-Rab7(DN)
****
****
****
****
Control shRNA
CPAP shRNA
Control shRNA
CPAP shRNA
Control shRNA
CPAP shRNA

Fig. 4

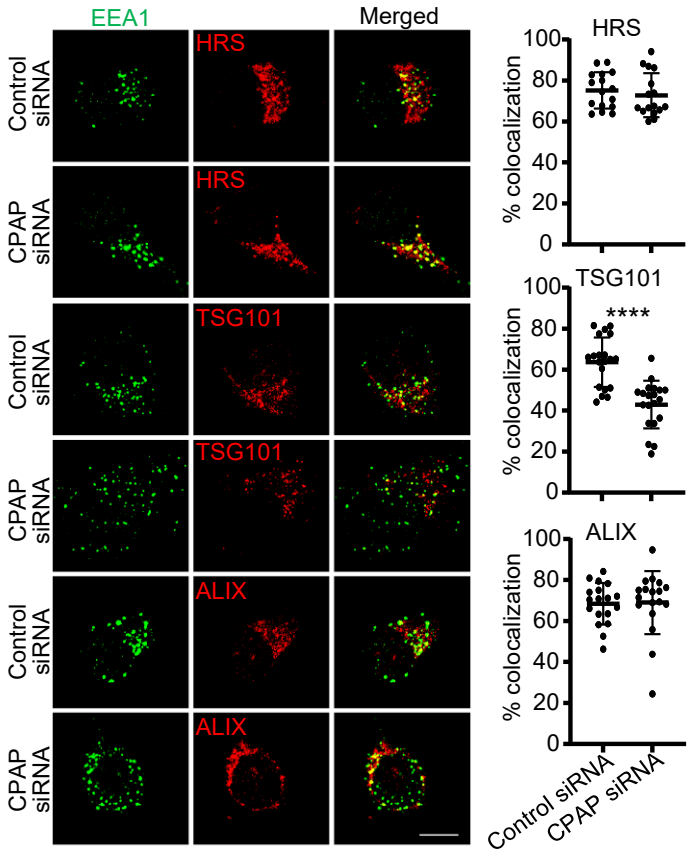
EEA1
Merged
HRS
TSG101
ALIX
Control siRNA
CPAP siRNA
% colocalization
100
80
60
40
20
0
****
Control siRNA
CPAP siRNA

Fig. 5

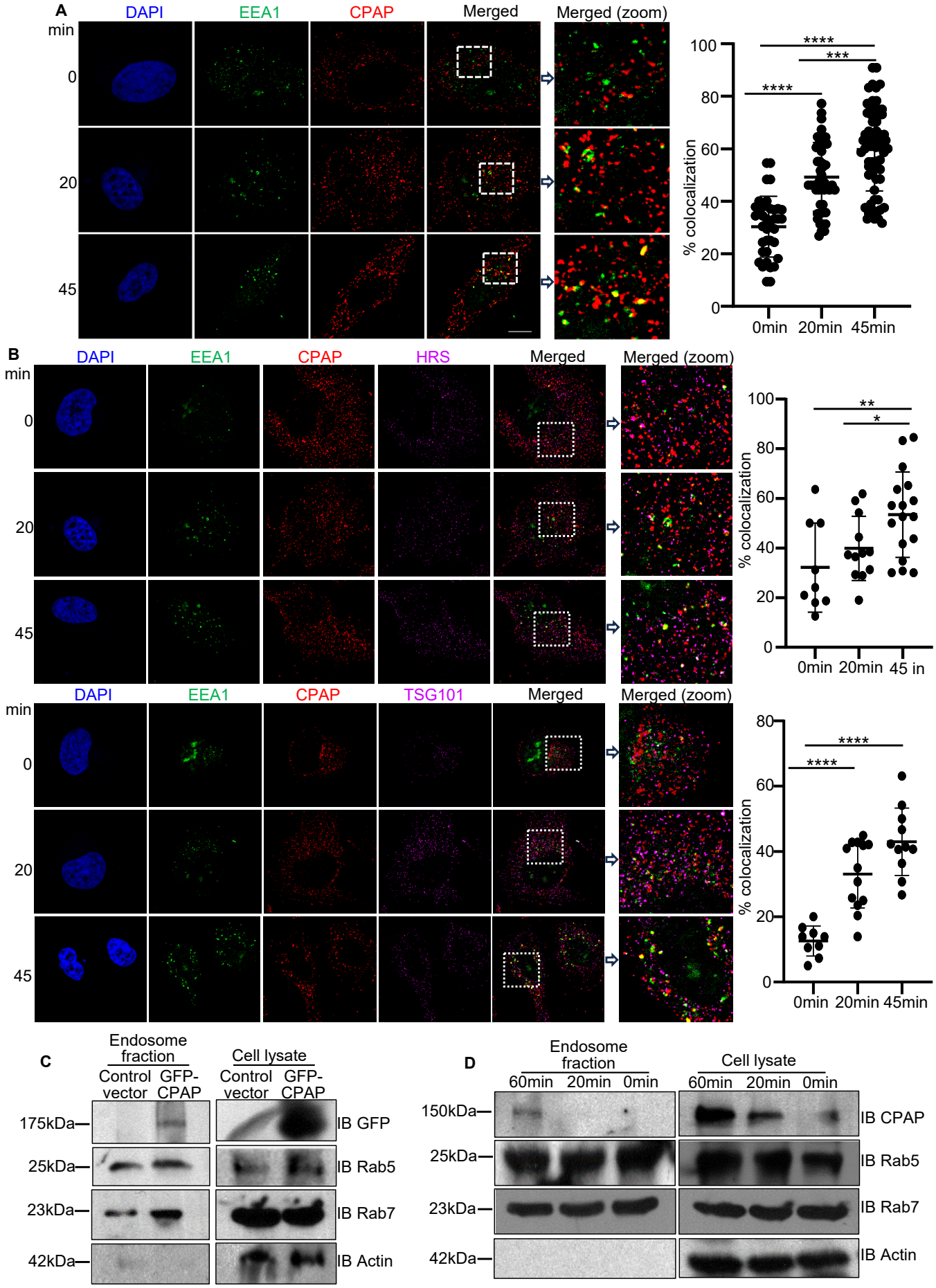
A
DAPI
EEA1
CPAP
Merged
Merged (zoom)
min
0
20
45
% colocalization
0min
20min
45min
****
***
B
HRS
TSG101
45 in
**
*

C
Endosome fraction
Cell lysate
Control vector
GFP-CPAP
175kDa
25kDa
23kDa
42kDa
IB GFP
IB Rab5
IB Rab7
IB Actin
D
60min
20min
0min
150kDa
IB CPAP

Fig. 6

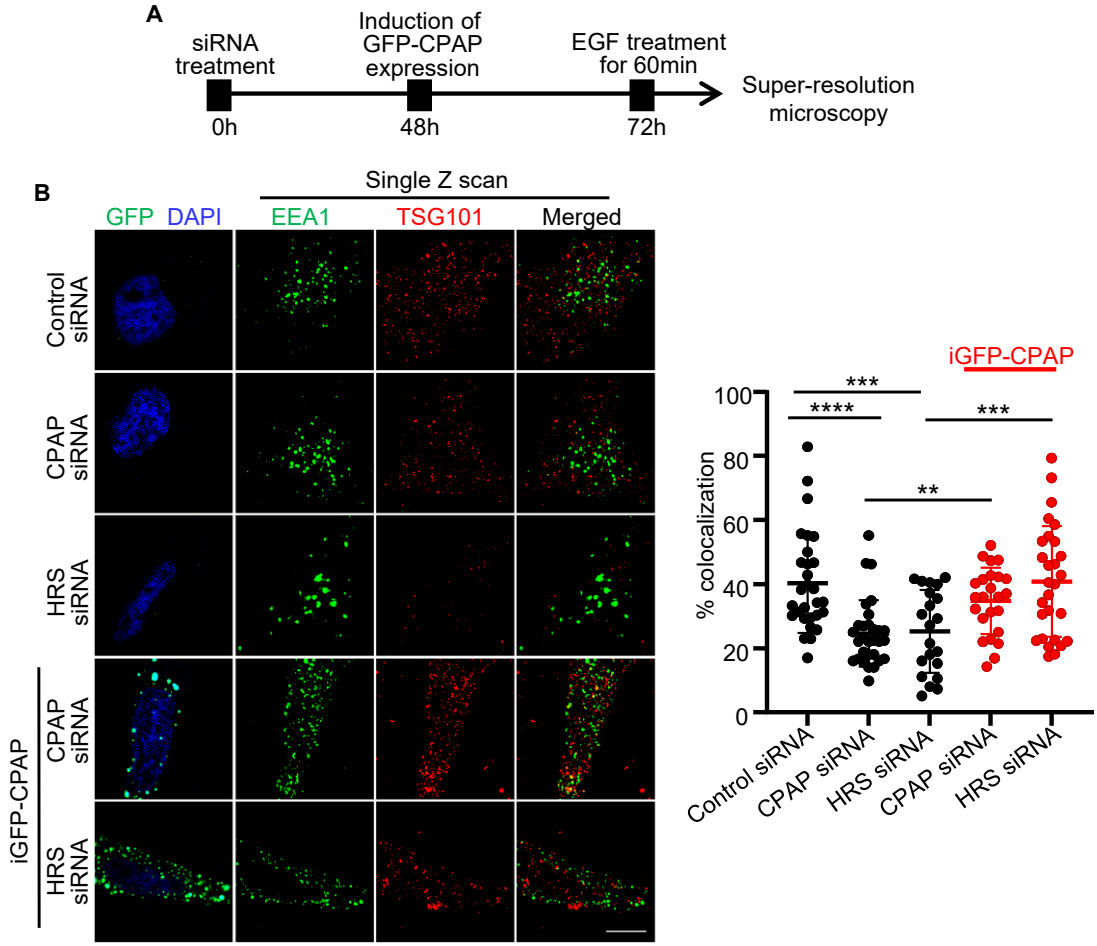
A
siRNA treatment
0h
Induction of GFP-CPAP expression
48h
EGF treatment for 60min
72h
Super-resolution microscopy
B
Single Z scan
GFP DAPI
EEA1
TSG101
Merged
Control siRNA
CPAP siRNA
HRS siRNA
iGFP-CPAP
CPAP siRNA
HRS siRNA
iGFP-CPAP
% colocalization
100
80
60
40
20
0
***
****
***
**
Control siRNA
CPAP siRNA
HRS siRNA
CPAP siRNA
HRS siRNA

Fig. 7

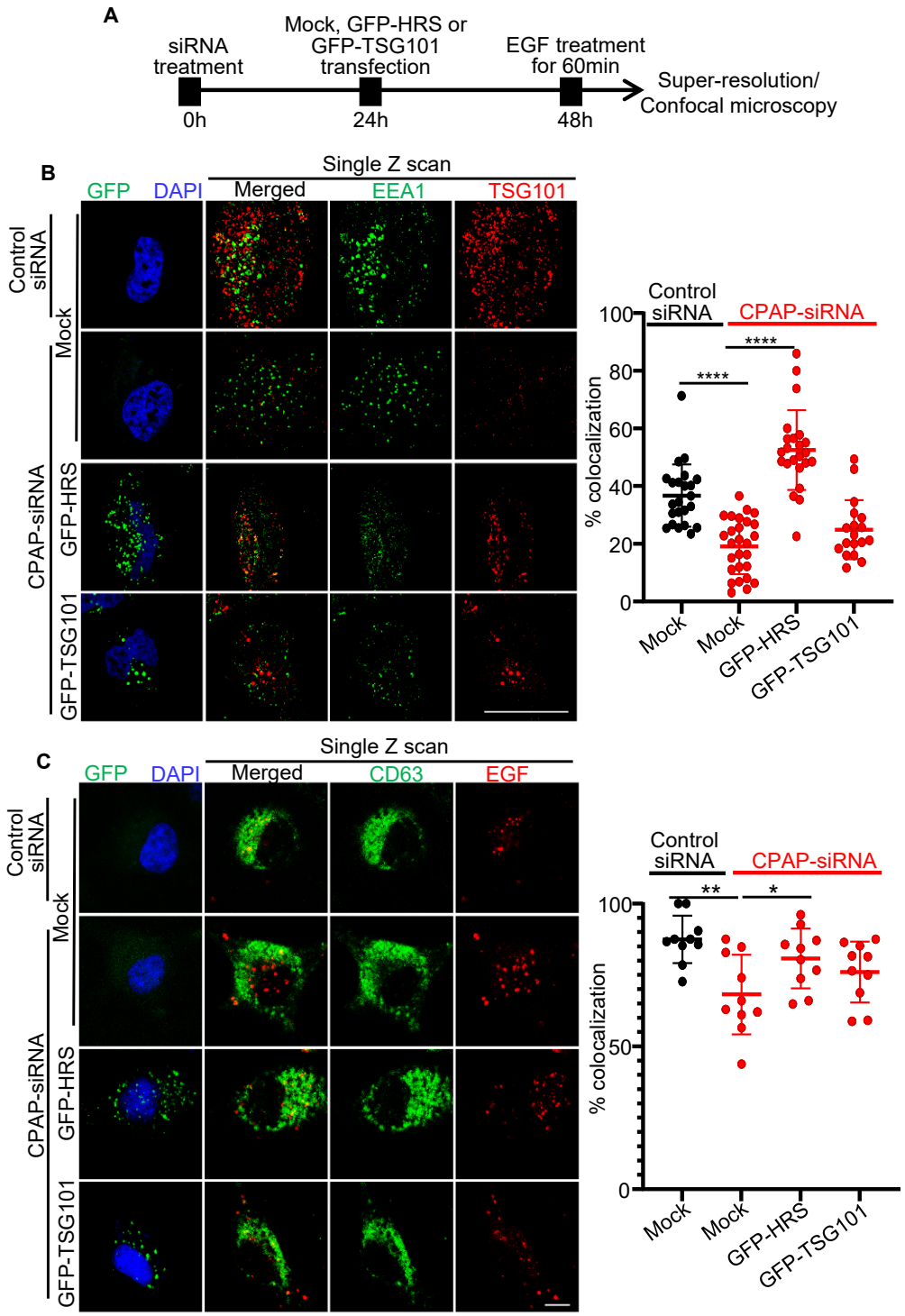
A
siRNA treatment
Mock, GFP-HRS or GFP-TSG101 transfection
EGF treatment for 60min
Super-resolution/ Confocal microscopy
0h
24h
48h
B
Single Z scan
GFP
DAPI
Merged
EEA1
TSG101
Control siRNA
Mock
CPAP-siRNA
GFP-HRS
GFP-TSG101
Control siRNA
CPAP-siRNA
% colocalization
100
80
60
40
20
0
****
****
Mock
Mock
GFP-HRS
GFP-TSG101
C
Single Z scan
GFP
DAPI
Merged
CD63
EGF
Control siRNA
Mock
CPAP-siRNA
GFP-HRS
GFP-TSG101
Control siRNA
CPAP-siRNA
% colocalization
100
50
0
**
*
Mock
Mock
GFP-HRS
GFP-TSG101

Fig. 8

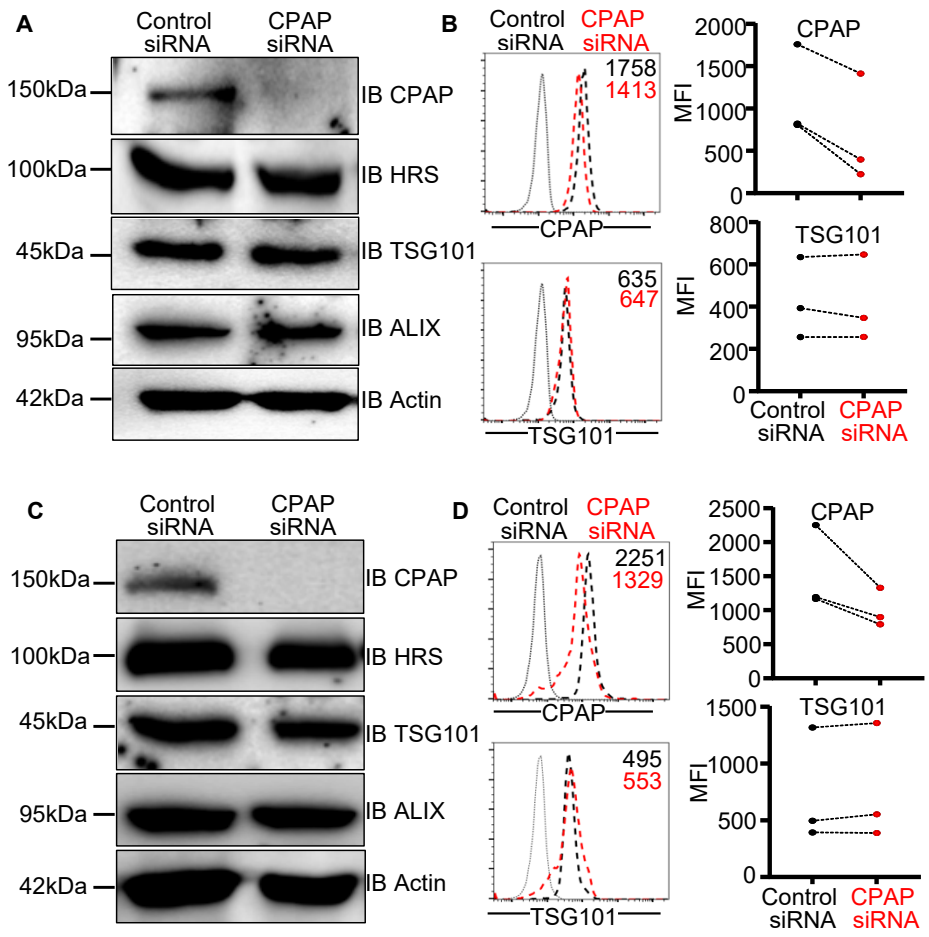
A
Control siRNA
CPAP siRNA
150kDa
100kDa
45kDa
95kDa
42kDa
IB CPAP
IB HRS
IB TSG101
IB ALIX
IB Actin
B
Control siRNA
CPAP siRNA
1758
1413
CPAP
635
647
TSG101
MFI
2000
1500
1000
500
0
800
600
400
200
C
D
2251
1329
495
553
2500

Fig. 9

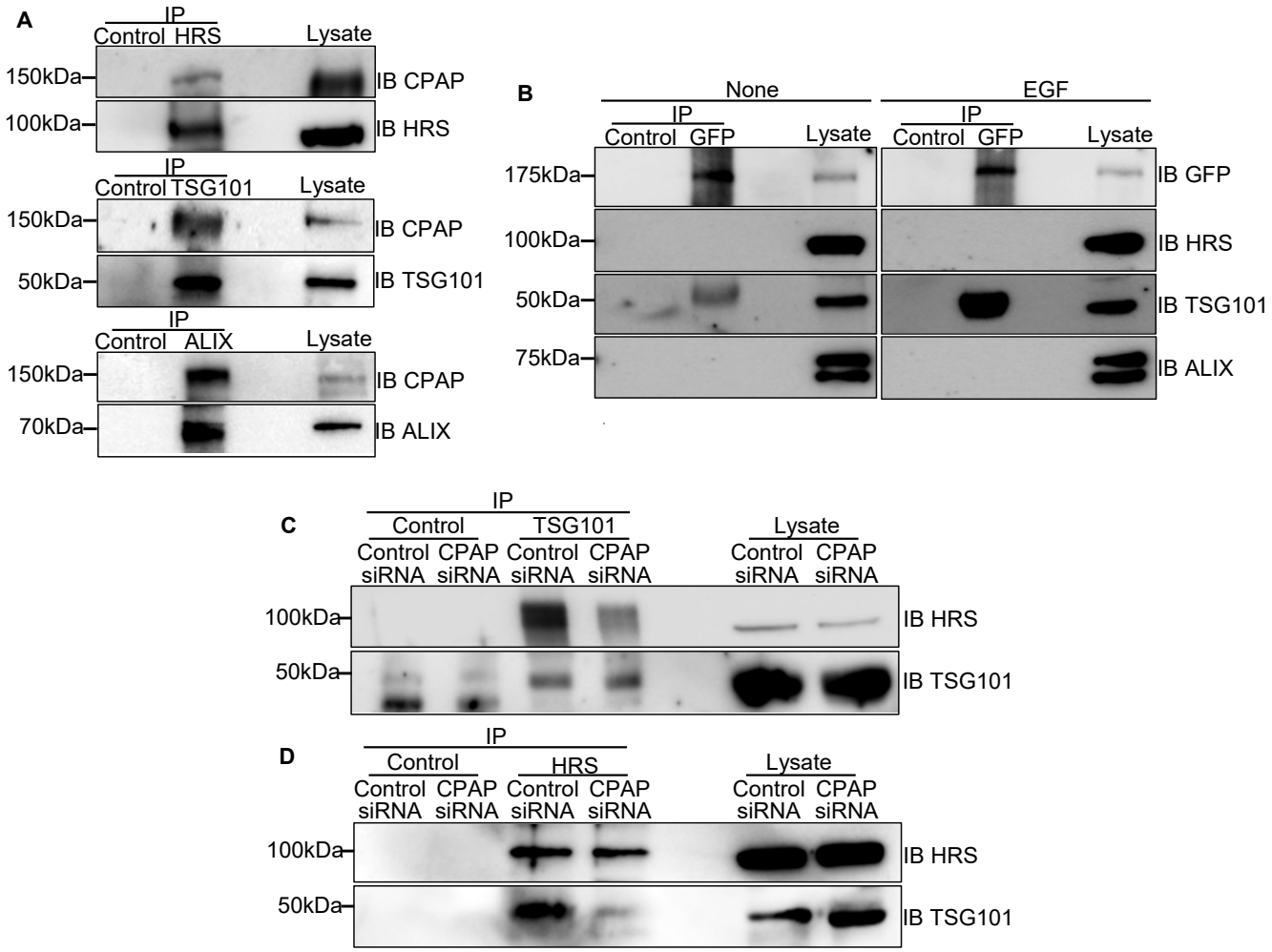
A
IP
Control HRS
Lysate
150kDa
IB CPAP
100kDa
IB HRS
IP
Control TSG101
Lysate
150kDa
IB CPAP
50kDa
IB TSG101
IP
Control ALIX
Lysate
150kDa
IB CPAP
70kDa
IB ALIX
B
None
EGF
IP
Control GFP
Lysate
175kDa
IB GFP
100kDa
IB HRS
50kDa
IB TSG101
75kDa
IB ALIX
C
IP
Control
TSG101
Lysate
Control siRNA
CPAP siRNA
100kDa
IB HRS
50kDa
IB TSG101
D
IP
Control
HRS
Lysate
Control siRNA
CPAP siRNA
100kDa
IB HRS
50kDa
IB TSG101

Fig.10

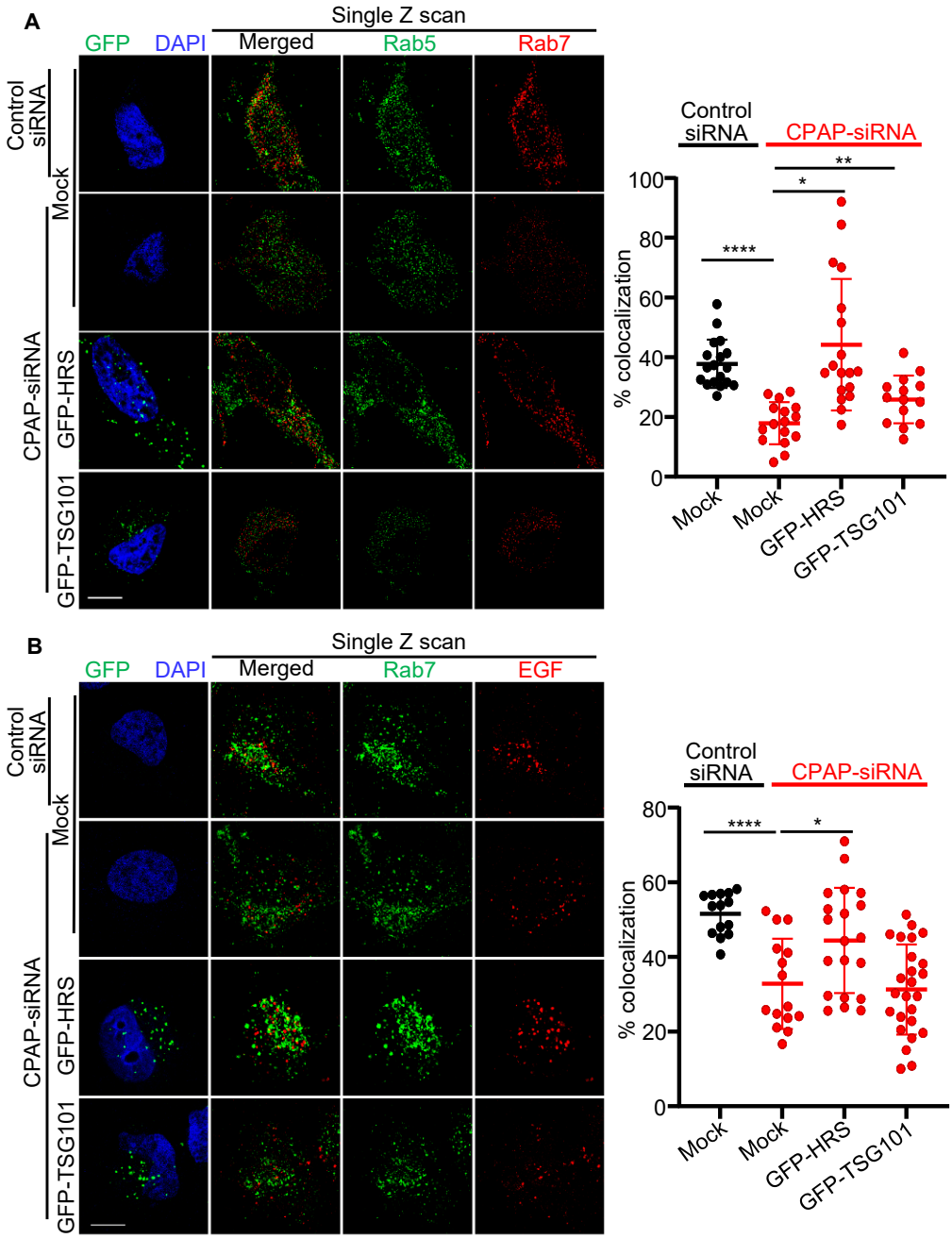
A
Single Z scan
GFP
DAPI
Merged
Rab5
Rab7
Control siRNA
Mock
CPAP-siRNA
GFP-HRS
GFP-TSG101
Control siRNA
CPAP-siRNA
% colocalization
100
80
60
40
20
0
****
*
**
Mock
Mock
GFP-HRS
GFP-TSG101
B
Single Z scan
GFP
DAPI
Merged
Rab7
EGF
Control siRNA
Mock
CPAP-siRNA
GFP-HRS
GFP-TSG101
Control siRNA
CPAP-siRNA
% colocalization
80
60
40
20
0
****
*
Mock
Mock
GFP-HRS
GFP-TSG101